The effect of co-liquefaction of organic solid waste with primary sewage on hydrochar yield and quality

HSM Nel

orcid.org/ 0000-0003-0397-476X

Dissertation accepted in fulfilment of the requirements for the degree *Master of Engineering in Chemical Engineering* at the North-West University

Supervisor:	Prof S Marx
Co-supervisor:	Dr RJ Venter
Graduation:	June 2025

Abstract

The continuous growth of the human population has increased energy demands globally as much as it has generated massive waste. Global energy demands are currently directed at alternative resources as fossil fuels are depleted, marginalised, and phased out due to environmental regulations. Waste generation and management has also become more intricate due to the rapid expansion and urbanisation taking place globally. The organic fraction of municipal solid waste (OFMSW) has a high energy potential. Due to its high moisture content, hydrothermal liquefaction is a viable option for converting it into renewable fuel sources. Hydrothermal liquefaction also relies on a solvent during the process, where water is usually added as a solvent to the reaction.

This study aimed to investigate sewage's effect as a solvent during the hydrothermal liquefaction of OFMSW. This included the effect it has on the yield and quality of the hydrochar. The objectives included preparing and characterising a synthetic mixture to represent the OFMSW during the investigation and determining the effect of liquefaction of sewage with OFMSW on the HTL product yields and quality. Lastly, the study was designed to determine the effect of HTL temperature and residence time on the hydrochar yield and quality when using sewage as a solvent during HTL.

The comparison between sewage and reverse osmosis water as solvent was made using a batch HTL process at 300˚C and 15 minutes of residence time. The various product yields were determined, and the products were characterised.

Substituting the water with primary sewage proved not to affect the yields of the various products. The hydrochar yields were (30.0 ± 1.7%) using deionised water as a solvent and (30.1 ± 2.6%) using sewage as a solvent. Bio-oil yields were (13.3 ± 1.8%) using deionised water as a solvent and (13.0 ± 0.6%) for sewage as a solvent. The calorific value of the hydrochar was similar, regardless of the solvent used, namely 30.4 ± 1.6 MJ/kg for water and 29.2 ± 0.7 MJ/kg for sewage. However, the ash of the hydrochars did differ as the sewage-derived hydrochar was slightly higher in ash than the hydrochar produced with water as solvent (5.0 ± 0.8 g/100g feedstock) vs (5.1 ± 0.2 g/100g feedstock).

The sewage did not significantly affect the yields of the biocrude oil, hydrochar and aqueous phase products although quality changes were noted namely a higher ash content in the biochar produced with sewage as solvent. Hydrothermal liquefaction allows for the simultaneous treatment of OFMSW and sewage, although secondary treatment of the aqueous phase must be

considered as bacteria were still detected. This allows for the generation of renewable energy sources and use case of two waste types, namely OFMSW and sewage.

Declaration of authorship

I declare that this report is a presentation of my own original work.

Whenever contributions of others are involved, every effort was made to indicate this clearly, by duly referencing the literature.

No part of this work has been submitted in the past, or is being submitted, for a degree or examination at this or any other university or course.

Signed on this, 2nd day of December 2021, in Potchefstroom.

_____

INITIALS AND SURNAME

Office: 0183892451

FACULTY OF EDUCATION **Cell: 0729116600**

Date: 4th December, 2021

TO WHOM IT MAY CONCERN

CERTIFICATE OF EDITING

I, Muchativugwa Liberty Hove, confirm and certify that I have read and edited the entire dissertation, **The effect of co-liquefaction of organic solid waste with primary sewage on hydrochar yield and quality** by **HSM Nel, orcid.org/0000-0003-0397-476X, student number 26182149,** submitted in fulfilment of the requirements for the degree **Master of Engineering in Chemical Engineering** at the **North-West University.**

HSM Nel was supervised by **Professor S. Marx** and co-supervised by **Dr. R. Venter**.

I hold a PhD in English Language and Literature in English and am qualified to edit such a dissertation for cohesion and coherence. The views expressed herein, however, remain those of the researcher/s.

Yours sincerely

Professor M.L. Hove (PhD, MA, PGDE, PGCE, BA Honours – English)

Acknowledgements

I would like to thank the following people and organisations for their contributions to the project:

- Prof. Sanette Marx my supervisor for her advice and guidance.
- Dr Roelf Venter and René Becker for assistance and support within the laboratory.
- The University of Johannesburg, Dr Christian Reinke and Orienda Sebabi for their assistance with the XRF and XRD analysis.
- My parents and loving support structure of friends during these uncertain and puzzling times.

TABLE OF CONTENTS

LIST OF TABLES

LIST OF FIGURES

1 Introduction

1.1 Background and Motivation

The continuous growth and development of the human population have increased energy demands globally; world energy demand is predicted to increase by 56% between 2010 and 2040 (Abomohra, et al., 2016). A model was proposed by Shafiee and Topal (2009) predicting that global reserves of oil, gas and coal would be depleted in approximately 35, 37 and 107 years. These predictions are outdated, and the number is everchanging as the development of new technology over the past years has made it possible to extract resources that were previously unknown or inaccessible (Kirsch, 2020). Although coal has the capacity to be used for many more years, a tremendous international effort is currently underway to phase out the use of coal for the generation of energy (Kirsch, 2020). In 2015 the United Nations agreed that the global warming limit must be kept below 2˚C as per the Paris agreement (United Nations, 2015). In 2018, the IPCC reported that to ensure the global warming limit stays below 1.5˚C, it is essential to phase out coal from electricity generation by 2050 (Zhao & Alexandroff, 2019).

The solution to ensuring energy security and global emission control is to exploit alternatives to fossil fuels. The two main alternatives are green and renewable energy sources (Abomohra, et al., 2016). One of the most promising alternatives to fossil fuels is producing renewable energy from biomass (Abomohra, et al., 2016). This is because biomass is abundant and cheap and can be converted into different biofuels using thermo-chemical conversion (Abomohra, et al., 2016). These conversion processes include pyrolysis, liquefaction, gasification, and direct combustion. Hydrothermal Liquefaction (HTL) is one of the most attractive processes as it uses almost any organic matter as feedstock, and it does not need dewatering or dry feedstock (Gollakota, et al., 2018). Besides the dewatering aspect, it is more viable and scalable and offers higher conversion ratios than pyrolysis (Abomohra, et al., 2016). The HTL process produces bio-crude oil, biogas, solid residue and aqueous by-product through high temperatures and pressures (Akhtar & Amin, 2011).

First-generation biofuels are primarily derived from edible biomass like maize and sugarcane (Correa, et al., 2017). However, edible biofuel feedstock needs large agricultural areas and energy inputs which compete with food production, lower biodiversity, increase land clearing and water demand and contribute to pollution associated with harvesting and production (Correa, et al., 2017). The focus has thus shifted from first-generation feedstock to second and third-

generation feedstock that does not compete with traditional agriculture, such as non-edible feedstock or waste (Correa, et al., 2017).

Globalisation and rapid economic expansion have led to increased production of solid waste. The United States alone produces 71 million tons of organic waste; globally, 46% of all solid waste is organic (Pace, et al., 2018). Organic waste comprises of garden refuse, food waste, wood chips, paper, and pre-consumer food waste (DEA, 2018). A significant number of environmental policies demand the diversion of organic waste from landfills and for these to be used in alternative ways to reduce greenhouse gas emissions and generate alternative energy sources (Pace, et al., 2018). Using organic waste as feedstock during HTL could be one such alternative.

Hydrothermal liquefaction uses a solvent to convert organic fractions of biomass into renewable energy sources. Generally, this solvent is water at sub-critical conditions, which acts as a catalyst for specific reactions during HTL (Obied, et al., 2022). South Africa receives about 492 millimetres of rainfall annually and is classified as a water-scarce country (Steele & Schulz, 2012). Water scarcity and protection of water sources have also become global environmental concerns, and there is a dire urgency to use water responsibly (Paiboonudomkarn, et al., 2022). Due to improper treatment, effluent from sewage plants is the primary source of surface water contamination (Tang, et al., 2021). Primary sewage contains only 1-4% solids, and a possibility arises to use this primary sewage effluent as a solvent during the HTL process. Not only would the primary sewage act as a solvent, but the solids in the sewage are comprised of lipid, protein, carbohydrate, and lignin fractions which could contribute to the HTL process and its products (Obied, et al., 2022).

Hydrothermal liquefaction of organic waste and primary sewage would not only produce possible renewable energy sources. However, it could also satisfy the requirements of using this as a waste management tool for organic solid waste and municipal waste sewage.

1.2 Research Question

Does the use of primary sewage sludge as a solvent during HTL of the OFMSW significantly affect the yield and quality of hydrochar for different applications?

1.3 Aim and Objectives

1.3.1 Aim

The aim of this project is to investigate the effect of the co-liquefaction of organic solid waste and municipal sewage on the yield and quality of the products with a focus on hydrochar.

1.3.2 Objectives

The objectives formulated to meet the aim of this study are as follows:

- Preparation and characterisation of a synthetic mixture to represent the organic fraction of municipal solid waste (OFMSW);
- Determine the effect of co-liquefaction of sewage with the OFMSW on HTL product yield and quality;
- Determine the effect of HTL temperature and residence time on hydrochar yield and quality when using primary sewage as HTL solvent.

1.4 Project Scope

Organic waste, recreated in a laboratory, was used during hydrothermal liquefaction together with primary sewage sampled from a local wastewater treatment plant. The products generated during the hydrothermal liquefaction were characterised and compared to products formed under the same reaction conditions but using deionised water as solvent.

To ensure that the aim and objectives of the project were met, the following chapters comprise the dissertation:

Chapter 2 – Literature review: This chapter investigates and discusses the impact of globalisation and rapid economic expansion and the effects of waste generation. South Africa's organic waste is investigated relative to water scarcity as the country is prone to this challenge. Next, hydrothermal liquefaction is introduced and discussed, and the hydrochar formed during HTL is discussed, outlining its characteristics. Finally, the uses of hydrochar are discussed in the context of soil remediation, adsorption, and renewable solid fuel source.

Chapter 3 – Experimental setup and design: This chapter outlines the experimental setup and procedures that were followed during the experimental phase of the project. The various materials and chemicals used during the experimental phase are discussed, including the feedstock and

how it was recreated in the laboratory. The hydrothermal liquefaction process and setup are given as well as product recovery and separation. Lastly, the chapter provides the characterisation methods used to characterise the hydrochar, feedstock, and other products.

Chapter 4 – Results and discussion: This penultimate chapter discusses the results of the experimental phase. Firstly, the characterisation of the feedstock and comparison with real-world feedstock is discussed. Secondly, the results from the hydrothermal liquefaction comparing primary sewage and deionised water as solvents are given and discussed. The other products, namely the bio-oil and aqueous phase produced during these runs, are also given and briefly discussed. Finally, the effect of temperature and reaction time on the hydrochar yield and quality is presented and discussed.

Chapter 5 – Conclusion and recommendations: This final chapter concludes the project and the investigation. The project is summarised, and recommendations for future investigations are offered.

2 Literature review

This literature review investigates the problem of waste on a global scale as well as the local South African scale. It also provides an overview of hydrothermal liquefaction (HTL), what it is and the products formed during the process. The HTL process is investigated to ensure adequate knowledge of the process and its various products, and its feasibility as an alternative energy source.

2.1 South Africa's waste defined

Globalisation has exerted a tremendous global impact on humankind with several advantages but arguably just as many new challenges. Many of the economic, social, and environmental challenges exist and ever evolving strategies have to be produced to combat these challenges (Ouattara, 1997). One of the many global challenges created as a result of urbanisation is the concentration of domestic waste and sewage that demand responsible treatment and management thereof (Tang, et al., 2021).

Various factors influence waste generation, including but not limited to population growth, population density, the economy, disposable income, urbanisation, and globalisation (DEA, 2018). Population size, growth and density are all well understood as directly responsible for the generation of waste. It is therefore crucial to appreciate the fact that population growth influences waste generation not only in the immediate, but also in the long term (DEA, 2018). Population density is also a factor to consider as not only do more densely populated areas generate more waste which is a challenge, but the management of this waste is also more complex. These components exert significantly high pressure on waste management services (DEA, 2018).

It is estimated that South Africa generated 54.2 million tonnes of general waste in 2017 (DEA, 2018). The main contribution to this general waste was organic waste with a 56.3% contribution. Estimated organic waste generated in South Africa during 2017 was 30.5 million tonnes where 68.8% of this waste was landfilled (DEA, 2018). Organic waste is defined according to the Department of Environmental Affairs (DEA) as waste emanating from garden refuse, wood chips and bark, food waste, pre-consumer food waste, sugar bagasse, pulp, paper, and black liquor. Organic waste in itself is complex as it not only differs from country to country, province to province but also varies at different times of the year (DEA, 2018).

The South African government has proposed several initiatives to divert organic waste from landfill sites. One such restriction is for the control of disposal of garden waste onto landfill (DEA, 2018). It regulates the diversion of garden refuse to redirect 25% to different facilities such as composting and recycling. Other initiatives include waste management facilities like the one in the Western Cape that was constructed for R400 million. The plant handles 600 tons of general waste per day which it separates into organics, recyclables, and non-recyclables. The DEA's end goal is to ensure minimal amounts of waste end up on landfill sites and thus more initiatives are proposed and explored (DEA, 2018).

2.2 Land, water, and the environment

Landfill waste is a global problem but specifically in developing countries. Estimations that the world's urban population will exceed 6 billion people by 2045 point to the numerous challenges and constraints on developing countries in South America, Asia, and Africa (Rajoo, et al., 2020). One specific challenge arising from this population explosion is dealing with municipal solid waste. As previously discussed, solid waste is projected to only increase with an increase in urbanisation. In Asia, the solid waste produced in 2012 was 0.28 billion tonnes and this is projected to increase to 1.8 billion tonnes in 2025 (Rajoo, et al., 2020). Contributing to the problem for developing countries are the large amounts of waste that are exported to these developing countries from developed countries (Rajoo, et al., 2020).

South Africa generated 54.2 million tonnes of general waste in 2017 (DEA, 2018). It is estimated that in 2017 alone 32.6 million tonnes of general waste were disposed onto landfill sites; organic waste which made up the majority (62%) of the general waste (DEA, 2018). Waste management policies include the diversion of garden refuse from landfill sites in South Africa (DEA, 2018). This helps to prolong the lifetime of landfill sites by reducing organic waste which in turn reduces the amount of leachate and methane emissions (DEA, 2018). In South Africa as of July 2018 there were 2478 licensed waste management facilities with most of these situated in Gauteng and the Western Cape. Waste management facilities in South Africa are forced to undergo external auditing. These audits report on how facilities manage waste and their compliance to local law and environmental policies. During these audit reports in 2017, it was noted that 20% of the facilities did not comply with waste management policies and regulations. This non-compliance included landfills not being compacted daily, insufficient staff training, inappropriate personal protective equipment being used, and no leak detection inspections being done. It was also noted that 40% of sites did not do proper groundwater and surface water sampling and testing.

Furthermore, other parameters of the waste sites as well as leak detections were not being conducted or tested according to the audit reports (DEA, 2018).

Landfill waste gets decomposed over time, producing greenhouse gases and leachate due to water infiltration. Leachate pollution effects three parts of the environment, i.e. the lithosphere due to soil contamination, the atmosphere due to greenhouse gases, and the hydrosphere due to ground water contamination (Mepaiyeda, et al., 2020). The estimated greenhouse gas emissions from the South African waste sector increased by 59.8% from 2000 to 2010 and consisted of 18 773 Gg of CO_2 with the majority of the emissions originating from solid waste disposal and the rest from wastewater treatment (DEA, 2000-2010). Pollution from landfill sites poses a great threat to groundwater sources by introducing pollutants like nitrates, minerals, inorganic compounds, bacteria, and heavy metals. Groundwater is limited to purify itself like surface water due to its nature, so these pollutants pose a lasting threat on groundwater sources (Mepaiyeda, et al., 2020). The state of waste report concluded that 40% of landfill sites do not comply with proper testing and evaluation of pollution in the proximity of the landfill site (DEA, 2018).

South Africa receives about 492 millimetres of rainfall annually whereas the global average is 985 mm. it is therefore classified as a water scarce country. More problematic is the uneven distribution of South Africa's rainfall where some parts of the country have annual floods while others are drought stricken (Archer, et al., 2019). During 2015-2017 the Western and Eastern Cape regions experienced severe to extreme drought during the winter rainfall period (Archer, et al., 2019). This drought had a massive impact on agriculture as well as residential and economic activities (Archer, et al., 2019). As a result, the agricultural sector had to reduce water usage, but more importantly, household and industrial sectors were restricted and fined for excessive water use (Archer, et al., 2019). The push for responsible water usage has dramatically increased in the region and in South Africa in particular.

2.3 Hydrothermal liquefaction

Recent changes in environmental regulations relative to climate change and the rapid depletion of fossil fuels have led to extensive research into biofuels. One of the most promising alternative fuels is the conversion of biomass to biofuel (Gollakota, et al., 2018). There are a few different ways to achieve this, namely, pyrolysis, transesterification, steam reforming and hydrothermal liquefaction (Gollakota, et al., 2018). The hydrothermal liquefaction (HTL) process is beneficial as it does not need dry feedstock resulting in higher overall energy recovery compared to other thermochemical processes (Bauer, et al., 2018).

Hydrothermal liquefaction of biomass seems very promising for producing not only renewable energy sources but also possible waste management. This is an area that has been greatly researched in recent years. The HTL process converts liquid or solid biomass into liquid and solid fuels. The process takes place between 523 to 647 K and 4 to 22 MPa (Gollakota, et al., 2018). The high temperatures and pressures ensure rapid hydrolysis and depolymerisation of the biomass which is followed by re-polymerisation, decarboxylation, and dehydration to produce bio-crude oil, hydrochar, process gas and an aqueous product (Bauer, et al., 2018).

The aqueous and hydrochar products are high in energy and have various possible applications or downstream uses (Swetha, et al., 2021). The aqueous phase can also not be discarded due to the possible negative environmental impact it poses (Buchun, et al., 2018). The aqueous phase contains between 10-40% of the energy in the original biomass. Discarding it would be uneconomical and unwise (Buchun, et al., 2018).

2.4 Hydrochar

2.4.1 Hydrochar and hydrochar production

Hydrochar is the solid product formed during the HTL process. It is like biochar but the term hydrochar is used to distinguish between the product formed from HTL and a different conversion method like pyrolysis. A vast majority of research is focused on the bio-oil product obtained from HTL as it is generally a more desired product. However, high yields and uses of hydrochar for a wide range of applications makes it a product that should not be overlooked. Applications for hydrochar range from soil remediation, bio-adsorbent and possible solid biofuel. Hydrochars generated under hydrothermal conditions are considered to be much better than other chars such as those produced during pyrolysis (Ponnusamym, et al., 2020). The reasons for this are that hydrochars generally have low amounts of heavy and alkaline earth metals and they are also high in volatile matter and functional groups which are beneficial if the hydrochar is to be used during adsorption (Ponnusamym, et al., 2020). Furthermore, the energy densification ratio (EDR) of hydrochars is very high, making it therefore an alternative favourable as a bioenergy fuel source (Ponnusamym, et al., 2020).

2.4.2 Hydrochar yield and physical characteristics

There are various factors that influence hydrochar yield. These include the type of thermochemical method, the type of feedstock and the process operating conditions. One such

example was observed by Biswas, et al. (2021) where reaction temperature, reaction time and solvent had a significant influence on product yields. The products formed during hydrothermal liquefaction and their quality and yields are strongly influenced by the cellulose, hemicellulose, lignin, protein, and lipid content of the feedstock (Zheng, et al., 2015). A strong correlation between lignin content of feedstock and hydrochar production have been observed with a high content resulting in a higher yield of hydrochar. At temperatures of 220˚C and higher, and in the presence of water, the lignin dissolves through hydrolysis (Ponnusamy, et al., 2020). This dissolved lignin is quickly converted into phenolic compounds like catechol, phenols, guaiacol and more via hydrolysis and de-alkylation. Finally, polymerisation reactions form solid residues resulting in the hydrochar (Ponnusamy, et al., 2020). Secondary hydrochar also gets formed from hemicellulose and cellulose via hydrolysis, followed by dehydration and finally polymerisation or condensation. In the case of cellulose, glucose is formed during hydrolysis and this can be converted into furfurals, phenols and HMF which are then polymerized into char (Ponnusamy, et al., 2020). Hemicellulose forms monosaccharides like xylose during hydrolysis and then furfural during dehydration and finally char during polymerisation. Hydrochar yield is thus very dependent on the amount of carbohydrates in the feedstock as these are broken down into various saccharides and components which are then polymerized into char (Hietala & Savage, 2021). This contrasts with bio-oil production which is more dependent on lipid and protein content.

Temperature also has a strong influence on hydrochar yield. At high temperatures the polymers are degraded, and thus solid-solid reactions do not occur as strongly as they would with lower temperatures (Ponnusamym, et al., 2020). Residence time, which does not include the heating and cooling time, and only the time at which the reaction is a target, temperature also has an influence on product formation and yield. Degradation takes time to take place and with short residence times it is often incomplete, but this shortened time does improve hydrochar polymerisation (Miao, et al., 2012).

Hydrochar pore sizes and volume have been studied and found to be lower compared to pyrolysis biochar (Ponnusamym, et al., 2020). Average pore size was found to be between 18 and 36 nm (Ponnusamym, et al., 2020). The International Union of Pure and Applied Chemistry (IUPAC) defines pore sizes of 2 nm or less as micropores, 2-50 nm as mesopores and 50 nm and above as macropores. Thus, HTL hydrochar is a mesoporous substance with some macropores present (Leng, et al., 2015). Ash content in hydrochar can range greatly from as low as 0.02 to a high of 71%. Leng, et al. (2015) found an ash content of 71% in hydrochar derived from sewage sludge

and attributed this to the high amounts of metal oxides and chemical particles present in the feedstock.

2.4.3 Hydrochar chemical properties

During hydrothermal liquefaction, biomass undergoes various reactions like deoxygenation and dehydration. These can be observed by the change in the H/C and O/C ratios. Biomass generally retains carbon but loses oxygen and hydrogen during the degrading and deoxygenation reactions that take place during the thermochemical process. Generally, hydrochar derived from HTL has a low H/C and O/C content (Ponnusamym, et al., 2020). This has been documented throughout literature. H/C and O/C content of HTL hydrochar is generally lower than pyrolysis char, lignite, and bituminous coal as displayed in table 2-1 taken from Ponnusamym, et al., (2020).

Table 2-1 : H/C and O/C ratios of hydrochars and coal sources

Hydrochar / coal source	H/C ratio	O/C ratio
L. Hyperborea	0.07	0.15
Oedogonium	0.07	0.10
Pinewood	0.06	0.57
Pongammia pinnata de-oiled cake	0.04	0.21
Sewage sludge	0.08	0.64
Lignite coal	1.08	0.22
Anthracite coal	0.34	0.07
Bituminous coal	0.8	0.22

It is evident that generally HTL hydrochar has a low H/C content and somewhat low O/C content in the case of most chars lower than lignite and bituminous coal. Some of the HTL hydrochars have much lower O/C and H/C content than the lignite and bituminous coal which is beneficial if the char is to be used as fuel source since low O/C and H/C content leads to a reduction in smoke and energy loss during combustion (Ponnusamym, et al., 2020).

Hydrochars produced from HTL are also high in oxygen-containing functional groups. These hydrochars contain different functional groups including hydroxyl, phenol, carboxyl, and carbonyl (Liu & Zhang, 2011). Temperature has been shown to have an influence on the number of functional groups in hydrochar. Leng, et al., (2015) found that functional groups were 1.5 times less in hydrochar produced at 360 ˚C than at 280 ˚C.

2.4.4 Soil remediation

Biochar is considered a multi-beneficial product when implemented as an agricultural soil ameliorant. Applying biochar for agricultural use can adjust the soil structure, improve physicochemical properties, and enhance the soil by adding various nutrients essential for plant growth (Yuan, et al., 2019). It can also possibly adsorb various contaminants from the soil like organic matter and heavy metals. Biochar also modifies the habit of microorganisms. The biochar not only adds possible nutrients to the soil for plants but also for microorganisms in the soil. Elements derivative from biochar like carbon, nitrogen and potassium are all beneficial to microbes in agricultural soil (Jianyun, et al., 2017).

Typical soil remediation methods can be classified as physical, chemical, and biological. Physical and chemical methods depend on the removal of toxins by effects of immobility, redox, electrodynamics and thermal treatment. These methods are not very suitable for arable soil as the processes are complex and come with high costs when done on a large scale (Yuan, et al., 2019). Biological remediation is based on microbes and plants that are both cheap and feasible but are extremely vulnerable to their surroundings and thus not very stable (Yuan, et al., 2019). Based on this observation, a cheap and reliable alternative is required. It is also crucial to understand that soil contamination migrates from soil to most agricultural plants thus posing a threat for human consumption.

Biochar can improve the physicochemical properties of degraded soil. Biochar has an ability to retain soil water which depends on the porosity and surface functionality of the biochar (Suliman, et al., 2017). Biochar increases the soil’s porosity due to its porous structure thus increasing the overall surface area of the soil and increasing the water retention properties of the soil. Furthermore, it was discovered that charcoal site soils which are a primitive biochar like soil have higher infiltration rates than regular soils. Infiltration is the process where water penetrates the ground and enters the soil. The higher infiltration rates suggest a possible decrease in overall soil erosion due to a decrease in overland flow (Glaser, et al., 2001).

Biochar also has the potential to improve chemical properties of the soil like pH, organic carbon, exchangeable cations also known as cation exchange capacity (CEC) and fertilising nutrients. Harvesting and fertilisation acidifies the soil which in turn influences the uptake and distribution of positively and negatively charged ions (Agegnehu, et al., 2017). The general practice is to add agricultural lime to soil in order to raise the pH levels which allows plants to grow to their maximum potential. Studies have shown that biochar raised soil pH to about a third of the rate of lime but also adds beneficial calcium and reduced aluminium toxicity on red ferralitic soils (Agegnehu, et al., 2017). The pH of various biochars differ depending on the reaction conditions as well as the feedstock used to produce the biochar. Biochars produced from manure and animal-product are rich in nutrients when compared to biochars derived from plant material (Albuquerque, et al., 2014).

Biochar also prevents leaching of valuable nutrients from the soil. The use of Brazilian pepperwood derived biochar reduced the amount of nitrate, ammonium, and phosphate leachate in soil by 34%, 34.7% and 20.6% (Yao, et al., 2012).

2.4.5 Hydrochar as adsorbent

Due to the various physical and chemical properties of biochar produced from hydrothermal liquefaction, it has the potential to be used as an adsorbent. Furthermore, the thermal stability of HTL hydrochar suggests less leaching of organic contaminants during the water treatment processes (Leng, et al., 2015). Various applications exist for biochar as adsorbent including but not limited to wastewater treatment, dye removal, metal adsorption, adsorption of organic pollutants from soil, pharmaceutical wastewater treatment, and pesticide removal from soil to list a few (Dai, et al., 2019).

Increase in antibiotic production for both humans and animals has led to an increase in pharmaceutical wastewater containing antibiotic contaminants. These contaminants influence the environment and persist in the environment for years due to transformation and bioaccumulation (Dai, et al., 2019). Various studies have been conducted to remove a range of antibiotic contaminants from wastewater streams. One study was carried out using iron and zinc mixed with sawdust biochar to remove tetracycline. This specific study showed great promise for removing tetracycline in aqueous solution as a removal rate of 89% was achieved in three cycles only (Zhou, et al., 2017). Hydrochar derived from eucalyptus sawdust was used to investigate the capacity of removing nitroimidazole antibiotics. The hydrochar was impregnated with H_3PO_4 and

had a removal efficiency of 97.10% for metronidazole and 96.40% for dimetridazole (Dai, et al., 2019).

Dye removal has also gained significant attention with the growth in the textile industry. The industry produces an extreme amount of wastewater as 200 L of water is used per 1 kg of textile material and the majority of this water ends up as wastewater (Yaseen & Scholz, 2019). Dyes in wastewater end up in the environment and contaminate not only scarce natural water sources but also the soil. Concentrations of dye in wastewater differ highly from 10 mg/l all the way to extremes like 7000 mg/l depending on different industries. Generally, however, it ranges from 10-250 mg/l (Yaseen & Scholz, 2019). There are many ways of removing dye from wastewater, but adsorption is preferred by many scholars due to its high efficiency compared to other technologies (Dai, et al., 2019). Commercially activated carbon is used to remove dye from effluent and although it is superior to other technologies, it is limited due to the high cost associated with this process (Ponnusamym, et al., 2020). HTL hydrochar derived from lignocellulosic biomass was found to be only slightly lower than that of commercial grade activated carbon (Leng, et al., 2015). The same study further found that HTL hydrochar outperformed pyrolytic biochar when used in dye adsorption. The HTL derived hydrochar had an adsorption capacity of 128.6-160.5 mg g^{-1} while the pyrolytic biochar only had a capacity of 12 to 130 mg g^{-1} (Leng, et al., 2015).

Heavy metals in wastewater streams also present numerous problems to the environment. Recently a lot of attention and research has been garnered with the utilisation of biochar to reduce heavy metal contaminants. Based on the form of the biochar, metals can be removed through physical sorption, complexation, precipitation, and electrostatic interactions (Ponnusamym, et al., 2020). The main focus of research has been on pyrolytic high temperature biochar but the problem with biochars generated at high temperatures is in the loss of volatiles and an increase in ash content (Ponnusamym, et al., 2020). They do, however, have high surface areas due to meso and micropores that characterise biochar. Another benefit from high temperature biochar is that functional groups useful in dye and metal exchange are reduced (Ponnusamym, et al., 2020). HTL derived hydrochar consists of a large number of functional groups which are very beneficial if the biochar is used in dye or metal treatment of wastewater. Evidence of this was found when comparing HTL hydrochar to a pyrolytic one in the adsorption of copper metal (Liu, et al., 2010). The strong removal of heavy metals was primarily due to oxygen functional groups present on the hydrochar surface.

2.4.6 Hydrochar as a renewable fuel source

HTL produces hydrochar that has coal-like properties and is therefore an attractive fuel source, but it is evident from the big variation in physical and chemical properties that not all HTL derived hydrochars are suitable as fuel sources. Some hydrochars have excellent higher heating values (HHV) compared to others. Most hydrochars are better than traditional coal fuel sources when comparing the higher heating values.

Table 2-2 : HHV of hydrochar derived from various feedstocks

Hydrochar	HHV (MJ kg^{-1})	Reference
Nannochloropsis sp.	13-21	(Reddy, et al., 2016)
Chlorella sp.	9-21	(Reddy, et al., 2016)
G. sulphuraria	24.51	(Dandamudi, et al., 2021)
Teak wood	26.76	(Alper, et al., 2021)
Cocos nucifera coir	31	(Gundupalli & Bhattacharyya, 2021)
Cocos nucifera pith	22	(Gundupalli & Bhattacharyya, 2021)

From Table 2-2 it can be observed that the HHV of different HTL derived hydrochars vary highly. It depends not only on the feedstock used but also the reaction conditions as discussed earlier. In the case of *Nannochloropsis* and *Chlorella* algae being used as feedstock, it was found that higher reaction temperature decreased the higher heating value and that a higher HHV was obtained at lower reaction temperatures (Zheng, et al., 2015). It is, however, clear that the higher heating value of some hydrochar is just as good and even better than traditional coal sources, making it a viable alternative to traditional fuel sources. Furthermore, the low nitrogen and sulphur content of some hydrochars produced from HTL are also beneficial as they have a very low negative effect of NOx and SOx pollution as in the case where swine carcases were used as feedstock (Zheng, et al., 2015).

2.5 Effect of temperature, reaction time and pressure on HTL process

As briefly discussed earlier, reaction conditions, including reaction time, temperature, and pressure, influence the products from hydrothermal liquefaction. Temperature and residence time are both critical parameters of the process that influence and define the products (Swetha, et al., 2021). Temperature directly influences biomass conversion during hydrothermal liquefaction, where an increase in temperature results in an increase in biomass conversion (Swetha, et al., 2021). In a study conducted by Carpio, et al. (2021), the effect of temperature on the hydrothermal liquefaction of algal biomass was investigated. Carpio, et al. (2021) observed an increase in biocrude oil formation with an increase in reaction temperature from 260˚C to 300˚C. The opposite was observed for the hydrochar yield, as it decreased with an increase in reaction temperature. It is understood that this is due to an increase in water-soluble products formed by the hydrolysis reaction at higher temperatures. Hydrolysis and these water-soluble products result in biocrude oil conversion. Reaction time is also a condition that influences the products during HTL. Residence time is the time that the reaction spends at the desired target temperature and does not include the heating or cooling time of the reactor. In the same study conducted by Carpio, et al. (2021), they found that at a reaction time of 0 minutes, some products had already formed but that 60% of the biomass was unconverted. It was then further observed that at a reaction time of 30 minutes, both the biocrude-oil and aqueous phase increased, but the solid residue or hydrochar decreased (Carpio, et al., 2021).

Fan, et al. (2022) concluded that residence time has slight effects on the bio-crude yield during HTL of sewage sludge. When considering the product yields and energy costs, typical times are between 5 and 30 minutes (Fan, et al., 2022). An increase in residence time typically leads to an increase in the bio-crude yields, but after a certain threshold, it leads to the opposite outcome (Fan, et al., 2022). Fan, et al. (2022) states that the increase in residence time allows the repolymerisation of oil fragments and this results in a decrease in bio-crude yield.

Pressure is another parameter that impacts the conversion of biomass into products during the HTL process. Bio-crude yield and quality have been thoroughly studied with the influence of pressure. The medium's phase is maintained by the subcritical, critical, or supercritical state (Fan, et al., 2022). The phase of the medium influences the rate of hydrolysis and biomass dissolution (Mishra & Mohanty, 2020). Increases in reaction pressure have been shown to have a positive effect on the bio-oil yield in some cases and the reverse effect in others (Yiin, et al., 2022). Once supercritical conditions are reached, it has been observed to have a small or insignificant

influence on the bio-crude yield (Mishra & Mohanty, 2020). Most HTL studies are conducted in the subcritical phases, which are below the critical pressure of water, namely 22 MPa (Yiin, et al., 2022). Malins, et al. (2015) concluded that the initial pressure of the H_2 atmosphere had an insignificant influence on the hydrothermal liquefaction of sewage and its products produced. The initial H_2 atmosphere in the study of Malins, et al. (2015) ranged from 2.0 to 11.0 MPa.

2.6 Effect of solvent on HTL process

Solvents have a significant effect on the products and hydrothermal liquefaction process. A study conducted by Biswas et al. (2021) using dried Azolla filiculoides with different solvents during HTL showed that alcoholic solvents improved bio-oil yield compared to using water. Biswas et al. (2021) used methanol and ethanol during HTL and obtained a high bio-oil yield of 28.7wt% and 28.9wt% using methanol and ethanol as solvents. HTL conducted using water only obtained a high yield of 21.5wt%. Ethanol has a hydrogen bond available and because this stabilises the HTL process leading to higher biomass depolymerisation (Biswas, et al., 2021). The higher yields are also primarily due to the alcoholic solvents having lower boiling points, lower critical points and the fact that they can generate more hydrogen than water during HTL. Solvent to feed ration during HTL influences product yield and quality of resulting products. Higher solvent ratios typically lead to improved hydrogen donation which enhances deoxygenation (I've even discussed this in my results) of the biocrude, this results in a higher quality product with reduced oxygen content. The biocrude is more energy dense and has a higher HHV. Increasing the ratio too much can dilute the biocrude reducing energy content (Jatoi, et al., 2022)

2.7 Hydrothermal liquefaction of sewage

Sewage sludge has been used throughout literature as feedstock for hydrothermal liquefaction. The sewage is not used in its raw state but rather a downstream sludge is generally collected and after further drying used in the HTL process (Silva, et al., 2020). Primary sewage typically contains only between 1-4% solids. It is important to note that throughout literature sewage sludge is pre-treated before hydrothermal liquefaction. The sewage sludge used throughout literature is first dried to remove the majority of the moisture present in the sewage. Silva, et al. (2020) dried sewage sludge at 105˚C for 24 hours prior to using it in the HTL process. Paiboonudomkarn, et al. (2022) pre-treated sewage sludge in an autoclave reactor prior to using it in the HTL process, the sludge was treated until the desired solid-to-liquid ratio was obtained.

Wide ranges of yields obtained during the HTL of sewage exist and are influenced by reaction conditions as previously discussed. Mishra & Mohanty, (2020) conducted experiments under conditions of 2 MPa as an initial pressure, temperature ranges from 275˚C to 350˚C, reaction time of 30 minutes and using sewage sludge as a feedstock. The sludge was pre-treated and had a moisture content of (4.6 ± 0.8 wt%). The hydrochar yields ranged from 8-14 wt% with the higher hydrochar yield obtained during the lower temperature runs (Mishra & Mohanty, 2020). Leng, et al. (2015) investigated the use of hydrochar derived from HTL of sewage sludge for the application of dye-adsorption. Leng, et al. (2015) prepared the feedstock according to Huang, et al. (2014). Huang, et al. (2014) pre-treated sewage sludge by firstly drying it in an oven at 105˚C for 24 hours and then grounding the dried sludge in a rotary cutting mill. Leng, et al. (2015) used the same preparation of the sewage sludge for HTL. Leng, et al. (2015) conducted experimental runs between 260˚C and 380˚C at a reaction time of 20 minutes and using acetone, methanol and ethanol as solvents. High hydrochar yields were obtained in the presence of these solvents as acetone yielded (48.65-53.12%), ethanol (46.29-50.41%) and methanol (45.38-51.22%). It was also observed that an increase in the reaction temperature from 260˚C to 320˚C had a decrease in hydrochar yield. The yields did however increase when temperatures were higher than 320˚C (Leng, et al., 2015). In a study by Adedeji, et al. (2022) beverage waste was co-liquefied with primary sewage. In this study sewage was not pre-treated or dried prior to the experimental runs. Besides the co-liquefaction of primary sewage with beverage waste a set of experimental runs were also conducted on the HTL of the primary sewage. The biocrude and hydrochar obtained was 14.8% and 4.1% respectively (Adedeji, et al., 2022).

The hydrochar produced during HTL from sewage sludge (SS) feedstock is high in ash and has a low HHV compared to the original feedstock. Du, et al. (2021) only obtained a HHV of 12.6 MJ/kg compared to the sewage sludge's HHV of 13.4 MJ/kg. The ash content of the hydrochar was also as high as 65.64% (Du, et al., 2021). Silva, et al. (2020) also obtained similar results when using SS as feedstock, the hydrochar obtained during their investigation had an ash content of 38.31% and the highest HHV obtained being 16.2 MJ/kg, only slightly better than the sewage sludge's HHV of 15.2 MJ/kg. Co-HTL is possibly a more favourable means of hydrothermal liquefaction of sewage sludge. Wang, et al. (2022) used sewage sludge and pinewood sawdust during co-liquefaction and produced a hydrochar with improved fuel quality. The hydrochar produced by Wang, et al. (2022) from sewage sludge had a very low HHV of 6.21 MJ/kg but when co-liquefied with pinewood sawdust, the hydrochar's HHV increased to 13.1 MJ/kg and also lowered the ash content from 55.91% to 33.54%. In the study by Adedeji, et al. (2022) beverage

waste and primary sewage was co-liquefied the HHV of the hydrochar was improved with co-liquefaction. The primary sewage had a HHV of 1

The following chapter presents a detailed account of the experimental process utilised in this study.

2.8 Pyrolysis and gasification

Thermochemical processes like gasification and pyrolysis are also used to convert biomass into bio-oil, biochar and gaseous products (Basu, 2010).

Gasification is the process that involves the partial oxidation of biomass feedstock at high temperatures in an oxygen-controlled environment or an environment where steam is present. Temperatures are usually between 700°C and 1500°C (Basu, 2010). This breaks down the biomass into syngas (CO_2, CO, H_2) and other gasses (Bridgewater, 2003)

Pyrolysis is a thermochemical process that operates in the absence of oxygen and at lower temperatures than gasification, usually between 300°C and 700°C (Basu, 2010). Pyrolysis decomposes biomass into biochar, bio-oil and a small amount of syngas (Bridgwater, 2003). The key distinction between gasification, pyrolysis and hydrothermal liquefaction is the operating conditions and resulting products. Gasification operates at higher temperatures with a controlled oxygen environment to produce syngas product and pyrolysis operates in an oxygen free environment to produce bio-oil and biochar as primary products.

Pyrolysis is useful with dry biomass feedstock, and it maximizes bio-oil yield it also has a lower reaction temperature compared to gasification making it more energy efficient (Slezak, Unyay, Szufa, & Ledakowicz, 2023). The main disadvantages of pyrolysis is that the bio-crude oil usually needs to be upgraded due to its high oxygen content and instability (Slezak, Unyay, Szufa, & Ledakowicz, 2023), it also needs a dry feedstock so if the feedstock is not dry it has to be dried prior to pyrolysis.

Gasification operates at high temperatures compared to the other two technologies and therefore a more complete conversion of the biomass occurs. This is beneficial as there is less solid residue and the syngas produced from the process can be easily used in energy generation (Patra & Sheth, 2015). During the high-temperature conversion impurities like tar form that require regular cleaning and maintenance, the process is also more expensive and complex to scale than pyrolysis (Patra & Sheth, 2015).

Hydrothermal liquefaction has the advantage over gasification and pyrolysis that it can use wet biomass as feedstock. The bio-oil component contains a lower oxygen content than compared to pyrolysis and is easier to upgrade (Ranjbar & Malcata, 2023). The extreme conditions needed for

HTL namely high pressure and temperature leads to a higher capital cost as well as it being difficult to scale the technology (Ranjbar & Malcata, 2023).

3 Experimental

This chapter details the materials, procedures and equipment used to carry out the experimental work. The materials used are described in section 3.1, the experimental setup is described in section 3.2, the hydrothermal liquefaction procedure and the separation process are presented in section 3.3, the separation and extraction of products are presented in section 3.4, and the characterisation techniques are presented in section 3.5.

3.1 Materials

The feedstock for the experimental procedures had to be constructed due to the inconsistent nature of organic waste. Secondly, sampling of municipal solid waste can be tedious and dangerous, so a constructed feedstock that can be replicated and reproduced is preferred. Deionised water and primary sewage were used as a solvent for the HTL reaction. The primary sewage was sampled at the wastewater treatment works of Potchefstroom. Table 3-1 gives the composition of the constructed feedstock.

Table 3-1 : Compounds of constructed feedstock

Compound	Composition in feedstock (mass %)
Fruits	19.97
Vegetables	17.07
Meat	6.56
Dairy	6.56
Sorghum	21.31
Oil	2.45
Roots and tubers	8.19

Garden refuse	11.85
Paper waste	6.22

The feedstock composition was determined from the annual state of waste report (DEA, 2018). The various components of the feedstock were locally sourced from grocers in Potchefstroom (GPS: -26.714, 27.104). Garden refuse consisted mostly of grass cuttings and leaves collected from garden services in Potchefstroom, Tuscany Ridge Estate (GPS: -26.667, 27.106) during February 2020. Paper waste consisted of three primary sources, namely, newspaper (3.7%), printing paper (72.88%), and corrugated paper (23.43%) (DEA, 2018). The composition of the fruits and vegetables in the feedstock was constructed based on research done at the University of Johannesburg that gave fruit and vegetable composition based on the colour of said fruits and vegetables (Ayeleru, et al., 2016). The various fruit and vegetable sources were dried and crushed to ensure that the breakdown of the fruits and vegetables occurred to a minimum. Table 3-2 shows the fruits and vegetables used in the feedstock and their respective % contribution to the fruit and vegetable amounts.

Table 3-2 : Fruit and vegetable composition

Component	Composition in fruit (%)
Green apples	32.23
Bananas	16.14
Berries	0.93
Red apples	26.08
Oranges	24.62
Component	**Composition in vegetables (%)**
Tomatoes	26.02
Carrots	23.42

Cauliflower	19.24
Lettuce	5.26
Red peppers	26.05

The roots and tubers stream in the feedstock was primarily only potato which was also dried and milled to ensure the quality of the product remained the same throughout the experiment procedure. The meat portion of the feed was broken down into protein and fat, substituted with soya protein powder "Just Protein" supplied by Health Connections Wholefoods. Pig fat was obtained from a local butchery. A milk powder was used to substitute the dairy component in the feedstock. Sunflower oil was used as the oil portion of the feedstock, and ground sorghum (Monati, Super Mabela) was used for the sorghum portion of the feedstock.

Table 3-3 gives a detailed list of other materials and chemicals used during the experimental runs and analytical processes.

Table 3-3: Chemicals used during the experimental phase

Component	Supplier	Purity (%)	Purpose
Acetone	Glass World	99.99	Used as a solvent during extraction and separation of products. Also used in cleaning of equipment used.
Deionised ultra-pure water	SG – ultra-pure water and reverse osmosis system from Labostar	-	Used as a solvent during certain HTL runs
Nitrogen gas	Afrox	UHP	Used to create an inert atmosphere for the HTL runs.
Potassium bromide	Sigma-Aldrich	≥ 99	Used as a blank sample during the FTIR analysis.

Nitric acid	ACE	70	Used in the ICP-OES as a mobile phase and inorganic adsorption sample preparation.
Formic acid	ACE	99.9	Used in the HPLC as a mobile phase and inorganic adsorption sample preparation.
Acetonitrile	Sigma-Aldrich	99.90	Used during HPLC as a mobile phase.

3.2 Experimental setup

A 945 mL stainless-steel autoclave batch reactor was used to conduct the hydrothermal liquefaction runs. A schematic representation of the reactor setup is given in Figure 3-1. The reactor has a removable stainless-steel cup with a nominal working volume of 750 mL. This cup makes adding feedstock and removing the product easier after the reaction is completed. The reactor is heated by a heating mantle connected and controlled by a controller. The controller ensures that the mantle supplies and maintains heat during the reaction. The reactor has a thermocouple to report the temperature inside the reactor and has a safety release valve that is spring-operated.

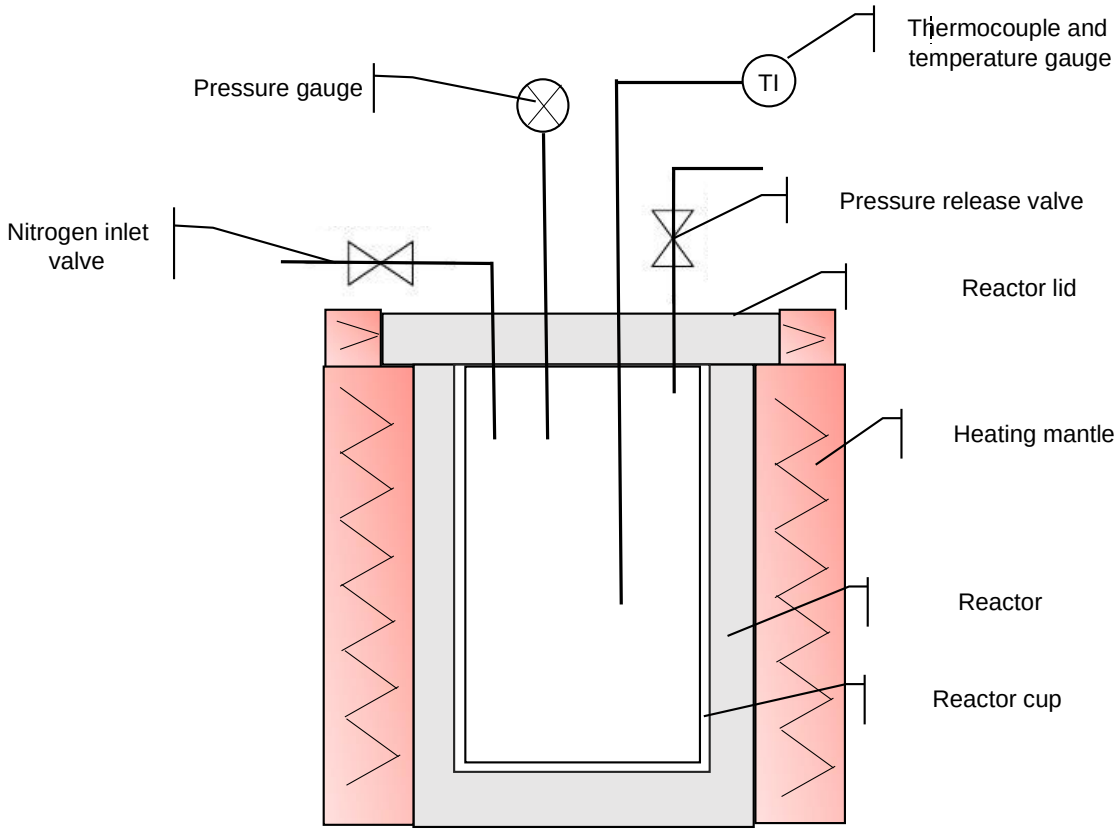

Figure 3-1: Hydrothermal liquefaction set-up

The extraction and separation of the products are done by first removing the product from the reactor cup. A metal spatula was used to remove the products in the cup by hand. To ensure all product and residue were removed from the reactor cup, the cup was rinsed with 50 mL of acetone. The products then undergo a regular Büchner vacuum filtration. During this filtration, solid residue is separated from liquid products by using filtration paper with pores that are small enough to ensure that solid particles do not filter through. The filter paper used was the Whatman ACE af Qualitative filter paper 28cm. Next, the solid residue is washed with acetone and dried in a convection oven. Next, the liquid product undergoes evaporation under reduced pressure in a vacuum evaporator which separates the acetone solvent from the bio-oil and aqueous phase product. This process is described in detail in section 3.4 below. Finally, the bio-oil and aqueous phase are cooled in an ice bath which solidifies the bio-oil, and the aqueous phase can be decanted.

3.3 Hydrothermal liquefaction

The stainless-steel cup was loaded with 86.8 g of dry feedstock, and then 112 g of deionised water or primary sewage was added to make up for the moisture content of the feedstock and to

serve as a solvent during hydrothermal liquefaction. The original moisture content of the feedstock was considered to determine the dry feed ratio to deionised water. The loaded cup was only loaded to 50% volume. Once water or sewage was added, the cup was well-stirred and agitated to ensure a homogenous mixture of the feedstock. The loaded cup was then placed inside the reactor.

The reactor was closed, sealed, and tested for leaks. The standard operating procedure of the reactor is attached as Annexure B. It is crucial for an inert reaction environment, and thus nitrogen was used to purge the reactor. After purging, the reactor was pressurised with nitrogen to a starting pressure of 1 MPa. Next, the heating mantle was attached and slowly ramped up to 550 ˚C until the desired reactor temperature was reached. The heating mantels are at a much higher temperature than the reactor due to being externally coupled mantles. The temperature inside the reactor was controlled to ±4˚C. The various reaction times and temperatures are presented in table 3-4 and table 3-5, including the solvent used for each reaction.

Different experimental runs were conducted. The first set of experiments that were conducted was to investigate the influence of using primary sewage as a solvent instead of deionised water. These experiments were the crux of the investigation and formed a proof of concept for future experiments and studies. Table 3-4 shows the conditions under which the comparison experiments were conducted. Three independent runs were done at each condition, totalling six runs to compare deionised water to sewage as a solvent.

Table 3-4 : Reaction conditions comparing sewage to deionised water

Solvent	Temperature (˚C)	Reaction Time (min)
Deionized water	300	15
Primary sewage	300	15

The second set of experiments that were conducted was to investigate the influence of reaction time and temperature on product yields and quality. These experiments were conducted using primary sewage as a solvent during the reaction. Table 3-5 below gives a summary of the various runs conducted under varying reaction conditions The initial pressure was 1 MPa for each reaction and was obtained by pressurising the reactor with inert nitrogen gas. The reaction

pressure was observed and is recorded in Annexure A. This pressure could not externally be influenced without changing the reaction conditions as is the case with this closed batch reactor.

Table 3-5: Varying reaction conditions using sewage as solvent

Solvent	Temperature (˚C)	Reaction Time (min)
Primary sewage	260	15
Primary sewage	280	15
Primary sewage	280	30
Primary sewage	280	45
Primary sewage	280	60
Primary sewage	300	15
Primary sewage	300	30
Primary sewage	300	45
Primary sewage	300	60

3.4 Separation and extraction of products

After the hydrothermal liquefaction reaction was completed, the reactor was left to cool down to a temperature of 30˚C as per the standard operating procedure. Next, the reactor was vented and reduced to atmospheric pressure. Once the reactor reached atmospheric pressure, the lid and the stainless-steel reactor cup were removed. The reactor sleave was weighed before and after the reaction to calculate the gas yield. The products were then collected in a beaker. The reactor cup was washed with 50 mL of acetone and decanted into the same glass beaker to ensure that all the product was collected. The next step was to do Büchner vacuum filtration, separating the solid and liquid phases. The washed 50 mL acetone and the product were added to the Büchner filtration. Now 450 mL of acetone was used to wash the solid residue in the Büchner funnel. The solid residue that remains in the Büchner is the yield of hydrochar from the reaction, and the aqueous product after vacuum filtration is a mixture of acetone, aqueous phase, and bio-oil.

3.4.1 Hydrochar drying

Once the Büchner filtration had been completed, the filter paper containing the hydrochar was placed in a Series 2000 Scientific oven at 60˚C for 3 hours. This was done to ensure that remaining residue acetone was evaporated from the hydrochar so that an accurate yield could be calculated. The filter paper was weighed, and the yield of the hydrochar was obtained. The hydrochar was then placed in an airtight container to ensure that no change in moisture could occur and analysis was done as soon as possible on the hydrochar.

3.4.2 Separation of bio-oil and aqueous phase

As discussed, earlier separation of the acetone from the bio-oil and aqueous phase components was achieved by conducting a rotary evaporation. This was done using the Buchi Rotovapor®R-300. Once the acetone had been separated from the bio-oil and aqueous phase mixture, it was discarded according to laboratory procedures. The bio-oil and aqueous phase mixture was then placed in an ice bath for 10-15 minutes. This causes the oil to become very viscous, almost solidifying. Once the oil has reached this state, the aqueous phase could be decanted and the separation of the aqueous phase and oil had been completed. The yields of both were then determined.

3.5 Analysis on the properties of hydrochar

Various analyses were done on the hydrochar to determine the physiochemical properties of the hydrochar produced during the HTL experiments. These analyses included proximate analysis, elemental analysis, scanning electron microscopy analysis (SEM), X-ray powder diffraction (XRD), X-ray fluorescence (XRF), and Fourier-transform infrared spectroscopy (FTIR).

3.5.1 Proximate analysis

Proximate analysis was done to determine the moisture, volatile matter, fixed carbon and ash of the hydrochar. The proximate analysis was done according to SANS 50:2011 for volatile matter and SANS 131:2011 for ash content. The moisture analysis was done according to SANS 5925:2007 and done by placing the samples in a Series 2000 Scientific oven. Finally, the ash content was determined by placing the samples in a muffle furnace following SANS 131:2011 to determine ash content.

Porcelain crucibles were used to house the samples during the proximate analysis. These crucibles were weighed to the nearest 0.1 mg and the initial mass of the crucible was recorded. The sample was heated in an oven at 105˚C until a constant mass had been reached, this was to ensure no final moisture was present. The loss of mass was used to calculate the moisture content of the hydrochar.

The volatile matter was determined using SANS 50:2011. The crucible and its lid (initial weight also recorded) were placed in a Carbolite Gero VMF 1000 furnace at 900˚C for 7 minutes. After cooling the crucible, its contents and the lid were weighed again to determine the volatile matter.

The ash content was determined using SANS 131:2011. The crucible and the sample within was placed in the furnace at 900˚C overnight and the remaining matter was determined to be ash.

3.5.2 Elemental analysis

The elemental analysis was conducted with accordance to ISO 29541:2010 method for solid mineral fuels. The carbon, nitrogen and hydrogen content were determined in the hydrochar samples by using a CE-440 elemental analyser by Exeter Inc. The SANS 17247:217 method was used as a standard during the elemental analyses

3.5.3 X-ray diffraction

The X-ray diffraction (XRD) of the hydrochar was done at the Central Analytical Facility of the Faculty of Science, University of Johannesburg, under the SPECTRUM department. The XRD analysis was done using the PANalytical X-PertPro X-ray Diffractometer. The XRD analysis was conducted to help identify the characteristics and the crystalline structure of the hydrochar.

3.5.4 X-ray fluorescence spectrometry

The X-ray fluorescence (XRF) analysis was also done at the Central Analytical Facility of the Faculty of Science, University of Johannesburg, under the SPECTRUM department. The XRF was conducted using the PANalytical MagiX PRO X-ray Fluorescence spectrometer. XRF was done on ash samples from the hydrochar to determine inorganic solid materials present in the hydrochar. This was done using the ISO 13605:2018 standard for solid mineral fuels to determine major and minor elements in coal ash and coke ash.

3.5.5 Scanning electron microscope (SEM) analysis

The surface of the hydrochar and feedstock was analysed using scanning electron microscopy (SEM) analysis. The SEM analysis was performed through a FEI Quanta FEG 250 electron microscope which was used for imaging of the hydrochar and feedstock surfaces. The samples were prepared before undergoing the SEM analysis. The samples were plated with a layer of platinum gold and placed on a carbon background to reduce the electrostatic effect and to ensure that the samples did not get too charged up. EDX was conducted on the samples using the Phenom Prox benchtop SEM

3.5.6 Fourier-transform infrared spectroscopy

The hydrochar was analysed by means of Fourier-transform infrared spectroscopy (FTIR) to determine functional groups present in the hydrochar. The samples were analysed with a Shimadzu IRAffinity Fourier transform infrared spectrophotometer. The spectra were determined across 4000-400 cm^{-1} wavelengths and at a resolution of 4 cm^{-1}. There were 45 scans done per sample and the results were processed using the IRsolution software. The hydrochar samples were ground with a pestle and mortar in a ratio of 1 to 100 with potassium bromide and then scanned with the apparatus.

3.5.7 Higher heating value analysis/Gross calorific value

The higher heating value was determined using a IKA C5003 calorific analyser. The analysis was done according to the SANS 1928:2009 ISO 1928:2009 standard. This same analysis was done to determine the calorific value of the feedstock and bio-oil.

3.5.8 Protein, fat, and carbohydrate determination

The protein, fat and carbohydrate composition of the feedstock was analysed during fibre analysis. This was done according to ASM 078 to determine the protein content and according to ASM 044 to determine the fat content. The total carbohydrates were determined according to ASM 075.

3.6 Analyses on additional products of oil and aqueous phase

To ensure that the effect of the solvent could be fully investigated, additional analyses were conducted on the bio-oil and aqueous phase products. This included high-performance liquid chromatography (HPLC), inductively coupled plasma optical emission spectrometry (ICP-OES),

and total phenolics for the aqueous phase. The analyses done on the bio-oil included gas chromatography-mass spectrometry (GC-MS), proximate analysis, Karl-Fischer analysis, elemental analysis, higher-heating values analysis, and total phenols.

3.6.1 High-performance liquid chromatography

Organic compounds that were present in the aqueous phase of the products was investigated by means of high-performance liquid chromatography (HPLC). The phenolics, acids and sugars were analysed by an Agilent Technologies 1260 Infinity II HPLC. An InfinityLab Poroshell 120 EC-c18 4.6 x 100 mm column was used in the HPLC. The HPLC-phenolics was done with two mobile phases present namely: A – 1% formic acid in water and B – 1% formic acid in acetonitrile. These mobile phases were mixed initially: 92% A and 8% B. At 10 minutes, they were mixed 70% A and 30% B. The operating temperature of the column was 40˚C and an injection volume of 10 µL was used with a Diode Array Detector. The detector used a wavelength of 275 nm and a bandwidth of 4 nm.

3.6.2 Inductively coupled plasma optical emission spectrometry

Inorganic compounds (Ca, K, Mg etc.) present in the aqueous phase were investigated by means of inductively coupled plasma optical emission spectrometry (ICP-OES). These compounds were quantified with an Agilent Technologies 725-ES ICP-OES with a radial torch. A 1% nitric acid solution was used during the ICP-OES as a mobile phase. Sample preparation was done by diluting each sample 10 times with the mobile phase in a centrifuge tube. This centrifuge tube was thoroughly mixed using a vortex mixer.

3.6.3 Gas chromatography mass-spectrometry

The bio-oil produced during the HTL process was analysed with gas chromatography mass-spectrometry (GC-MS). An Agilent Technologies 7890GC system with 5975C inert MSD was used to conduct the GC-MS. A 30m Agilent J&W VF-5ht Ultimetal column was used with a diameter of 0.25 mm and with a film of 0.2 µm thick. Helium at a flow of 13.3 mL/min as a carrier, it operates at 35˚C for 4 minutes, then at 190˚C for 5 minutes, and finally at 420˚C for 2 minutes. The samples were dissolved with acetonitrile. Qualitative analysis was done to determine which compounds were present in the bio-oil.

3.6.4 Microbiological analysis

Microbiological analysis was conducted on the primary sewage as well as the aqueous phase obtained from the hydrothermal liquefaction process. Samples were sent to Envirocare laboratory. Total Enterobacteriaceae count (TEC) was performed to identify and quantify the amount of bacterium present in the samples.

4 Results & Discussion

This chapter reports and discusses the results of the hydrothermal liquefaction experiments. The results include characterisation, mass and product yields and qualitative analysis of these product yields. Section 4.1 reports the characterisation of the feedstock used in the experimental runs. Section 4.2 discusses the results and comparison between the hydrothermal liquefaction runs using water and then sewage as solvent. Section 4.3 discusses the influence of temperature, and 4.4 focuses on the influence of time. Finally, section 4.5 reports the findings and characterisation of the hydrochar produced.

4.1 Characterisation

The constructed organic feedstock was characterised using fibre analysis, ether extraction to determine fats, carbohydrates, protein analysis, and proximate analysis.

The organic waste feedstock was 99.33% dry after the drying steps were taken. It had a total ash content of 4.18% and a higher heating value of 18.37 MJ/kg. The protein, carbohydrate and fat analysis had the following results as depicted in Table 4-1.

Table 4-1 : Protein, Fat and Carbohydrate content of feedstock

Component	Value (Mass %)
Protein	12.21
Fat	3.06
Carbohydrates	79.88

The elemental analysis of the organic feedstock showed carbon at 42.9%, hydrogen at 6.49% and nitrogen at 2.52%. The (C:N) ratio was 17.06, which is comparable to Olusola, et al., (2016) that obtained a (C:N) ratio of organic solid waste of 22.74. A 2016 study supported by the University of Johannesburg (Olusola, et al., 2016) conducted an elemental analysis on the organic portion of landfill waste that was collected from a landfill site in Florida, Johannesburg. The results from the elemental analysis are reported below in Table 4-2 and compared to the elemental analysis on the constructed feedstock used in this current investigation. This analysis was on a dry ash-free basis (DAF).

Table 4-2 : Elemental analysis and comparison with Florida landfill site

	Feedstock from Olusola, et al. (2016) (DAF)	Constructed organic feedstock (DAF)
Carbon (%)	45.03	42.90
Hydrogen (%)	6.20	6.49
Nitrogen (%)	1.98	2.52
Residual (%)	41.16	48.08

Furthermore, the proximate analysis yielded the following results that were also compared to the Florida landfill site waste (Olusola, et al., 2016). The results are compared in Table 4-3.

Table 4-3 : Proximate analysis comparison with Florida landfill site

	Feedstock from Olusola, et al. (2016)	Constructed organic feedstock
Ash (Mass %)	5.56	5.04
Moisture (Mass %)	63.47	59.17
Volatile matter (Mass %)	22.63	32.19
Fixed carbon (Mass %)	8.77	3.59

It is evident from the proximate analysis that the constructed feedstock and that of the landfill site are comparable. The moisture content is high in the feedstock, which coincides with organic material being high in moisture content. The moisture content (74.11%wb) of a wet sample of food waste taken by Ma, et al. (2016) was shown to be similar to the constructed organic feedstock and the Florida landfill waste. This high moisture content can be expected from waste containing many vegetables and fruits. A study by Komilis, et al. (2014) reported a carbon percentage of 39.5% (dry basis) which is once again comparable to the constructed feedstock and Florida landfill

waste. This is important when considering the HHV of the feedstock, as carbon is primarily responsible for energy content in biofuels due to the exothermic reaction with oxygen. A study by Wu, et al. (2021) where analysis was done on integrated gasification combined cycle of MSW, reported that the HHV value of their feedstock was much lower than that of coal, 13 MJ/kg compared to 30 MJ/kg. The correlation between the higher heating values can be drawn from each feedstock's carbon content, with the coal's carbon being 80% and the MSW's carbon content only being 30% (Wu, et al., 2021). It is also evident from the feedstock that the low higher heating value can be associated with the low initial carbon content of the feedstock as well as the high moisture content.

4.2 HTL with sewage and deionised water

The following phase of the study included investigating the effects of sewage compared to deionised water as a solvent. The aim was to determine if there are differences in product yield and product quality between using deionised water or sewage as a solvent during the HTL process. Although the focus of the research was on the hydrochar as desired product, the effect of replacing water as a solvent with sewage was also determined for the other HTL products that formed.

4.2.1 Overall yields and carbon balance

The hydrochar, bio-oil and gas yields that were obtained during the hydrothermal liquefaction of MSW with deionised water or sewage are compared below in table 4-4. As previously described, the gas yield was measured as the difference in weight before and after the reaction had taken place. This analysis was done on a as received (AR) basis meaning all the original moisture and ash was present in the sample.

Table 4-4: Comparative yields from HTL using deionised water or sewage as a solvent (As received basis AR)

Solvent type	Hydrochar yield (wt. %)	Bio-oil yield (wt. %)	Gas yield (wt. %)	Aqueous phase yield (wt. %)
Deionized water	30.0 ± 1.7	13.3 ± 1.8	19.8 ± 1.8	36.9 ± 1.4
Primary sewage	30.1 ± 2.6	13.0 ± 0.6	18.6 ± 2.1	38.3 ± 5.2

There is a slight difference in yields, but considering the experimental error on yields, namely 2.9% for hydrochar yield and 2.1% for bio-oil yield, it could explain the slight deviation. The carbon balance over all the runs conducted was 86.4%. More detail on the hydrochar yield is given under section 4.2.2.

4.2.2 Analysis of yields

A total of three runs were conducted with both deionized water and primary sewage as solvent to determine repeatability and the variance in the data. These are dry ash free (DAF) percentage yields determined on the DAF feedstock amount. By comparing the two solvents, it is observed that there is very little influence on the yield of the hydrochar and bio-oil. The yield obtained per kg of feedstock used is shown in Table 4-5 which further shows an insignificant difference in yields when comparing the two solvent types.

Table 4-5: HTL product yields on a DAF basis per kg of feedstock

Solvent type	Hydrochar yield (DAF g/kg feed)	Bio-oil yield (DAF g/kg feed)
Deionized water	300.1 ± 16.6	131.9 ± 19.4
Primary sewage	301.1 ± 26.5	128.2 ± 7.1

Yields obtained by Saengsuriwong, et al. (2021) using food waste as feedstock in ratios of 1:3, 1:5, and 1:7 with deionised water were roughly 15-20 wt. %. Higher bio-char yields and lower bio-crude yields were obtained during this investigation compared to that of Saengsuriwong, et al. (2021) this is likely due to the difference in feedstock used. The feedstock of Saengsuriwong, et al. (2021) contained more protein and lipid content than the feedstock in this study.

The very similar results obtained by using RO water or sewage as solvent are due to the high similarity between the two solvents. The primary sewage only had 2.25% solids, which is contrary to literature where sewage sludge is used during co-liquefaction. As is the case with Silva, et al. (2020) where the sewage sludge used during their experiments had a moisture content of 81% and was also then further dried prior to the HTL runs to ensure sufficient solids were present during the HTL process. The main substantiating factor between the experiments in this study and that of literature is the prior treatment of the primary sewage. As described above in literature

the primary sewage is pre-treated and dried to ensure that the feed used during the HTL process is low in moisture content, as is the case in Silva, et al. (2020).

Solvents could have significant effects on the yields of HTL products. This is the case with Biswas, et al. (2021), where the effects of C2H5OH (ethanol) and CH3OH (methanol) were profound compared to using water as a solvent. Alcoholic solvents gave an increased bio-oil yield compared to water. Ethanol having a free hydrogen bond means that the alcohol solvent stabilises the free radicals during HTL and results in higher biomass depolymerisation (Biswas, et al., 2021). This is, however, not the case when using primary sewage due to the high similarity to water. The increase in ash yield after combustion of the hydrochar that is produced using sewage in section 4.2.2 further supports this and is elaborated below.

4.2.3 Elemental and proximate analysis of hydrochar

The elemental and proximate analysis were performed on the hydrochar and feedstock and the corresponding results are shown in Table 4-6 and Table 4-7. The remaining portion of the elemental analysis was attributed to being oxygenated groups. The calorific value of the feedstock and hydrochars produced is also given in Table 4-7.

Table 4-6: Elemental analysis results of feedstock and hydrochar from different solvent

	Feedstock	Hydrochar with solvent deionised water	Hydrochar with solvent primary sewage
Carbon (%C)	42.9 ± 0.2	68.2 ± 0.1	68.1 ± 0.13
Hydrogen (%H)	6.5 ± 0.2	5.6 ± 0.2	6.0 ± 0.1
Nitrogen (%N)	2.5 ± 0.1	3.3 ± 0.5	3.4 ± 0.1
Residual (%R)	48.0 ± 0.3	22.9 ± 0.2	22.5 ± 0.2

Table 4-7 : Proximate analysis results of feedstock and hydrochar with different solvents

	Feedstock	Hydrochar with solvent deionised water	Hydrochar with solvent primary sewage
Ash (g/100g Feedstock)	5.0 ± 0.8	4.1 ± 0.8	5.1 ± 0.2
Moisture (g/100g Feedstock)	59.2 ± 4.0	0.8 ± 0.3	0.8 ± 0.1
Volatile matter (g/100g Feedstock)	32.2 ± 1.7	15.1 ± 0.4	15.4 ± 0.3
Fixed carbon (g/100g Feedstock)	3.6 ± 3.2	11.7 ± 0.9	10.3 ± 0.3
Higher heating value (MJ/kg)	18.4 ± 0.1	30.4 ± 1.6	29.2 ± 0.7

Besides the carbon content, the hydrogen and nitrogen content of the hydrochar and feedstock are very similar. There was an apparent increase in carbon content from the feedstock to the hydrochar after the HTL process. The decrease in the oxygen and hydrogen groups can be attributed to the breaking of functional groups by decarboxylation and dehydration reactions (Carpio, et al., 2021). Hydrogen and oxygen are expected to decrease during HTL due to the degradation of the biomass. Deoxygenation is an important reaction during HTL and occurs through either dehydration (H_2O) or as decarboxylation (CO_2 or/and CO) (Carpio, et al., 2021). An increase in deoxygenation occurs at high reaction temperatures up to 300˚C and is strongly influenced by reaction time and temperature (Carpio, et al., 2021).

The increase in fixed carbon content and lower oxygen content of the hydrochar compared to the feedstock led to a significant increase in the higher heating value from 18.4 MJ/kg to 29.2 MJ/kg and 30.4 MJ/kg, respectively. The energy density of both hydrochars is increased after the HTL process, indicating the densification of the biomass, this is also observed with the increase in fixed carbon content. The energy retention parameter indicates to what extent the energy in the original biomass feedstock was retained in the hydrochar (Lu, et al., 2013). This is a better comparison than just HHV as it relates to the amount of recovered hydrochar and the original biomass. The energy retention parameter of the two hydrochars was 0.50 for water as solvent and 0.48 for sewage as solvent.

The moisture content of both hydrochars was also significantly lower than that of the feedstock, and the volatile matter higher. This also positively contributed to the upgrading of the feedstock. As previously noted, the ash content of the hydrochar increased when sewage was used as the solvent type during the hydrothermal liquefaction process. This is observed throughout literature when using sewage sludge as feedstock during HTL. Once again, the sewage used here only contained 2.25% of solid matter hence the influence on the product.

At first, when comparing the ash results, it could seem that the ash from the sewage run is more than that of the feedstock and that the mass balance does not match. However, the ash in the primary sewage was analysed and found to be 0.48% (mass%) of the sewage. When considering the amount of sewage added as a solvent during the HTL process, an additional 0.63 g (which is 0.48 mass%) of ash is added to the mass balance. This mass balance of the ash explains why the increase in ash is observed in the proximate analysis of the hydrochar derived from HTL using sewage as solvent.

4.2.4 Surface morphology

The surface morphology of the hydrochar and the feedstock was observed using scanning electron microscopy (SEM). Energy dispersive x-ray (EDX) was also done to investigate the mineral composition of the hydrochar and feedstock. The surface of feedstock can be seen from the micrographs in Figure 4-1 and Figure 4-3. The surface of the feedstock can be seen as a mixture between fibrous strands and smooth folded surfaces. It is irregular in nature as could be expected with a mixture of cellulose and hemicellulose (Wang, et al., 2022).

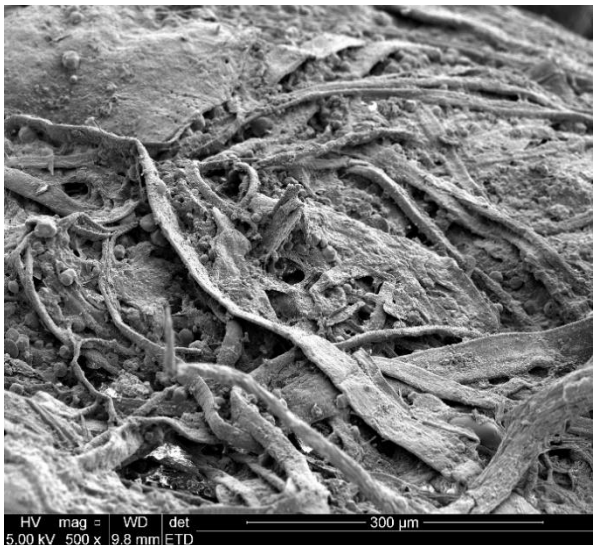

Figure 4-1: SEM of feedstock 300 µm

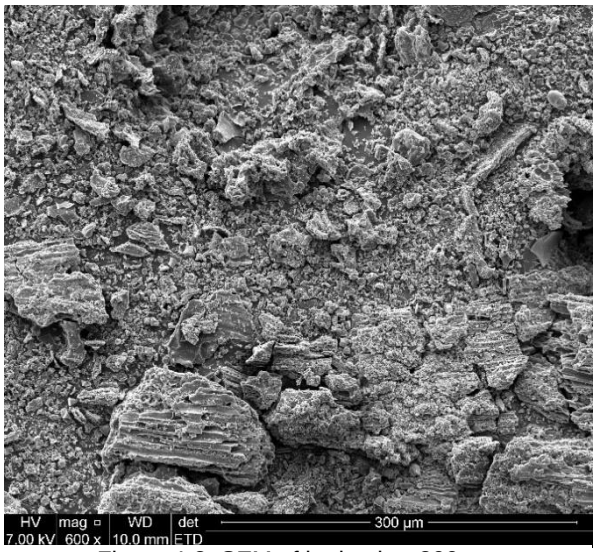

Figure 4-2: SEM of hydrochar 300 µm

Figure 4-3: SEM of feedstock 100 µm

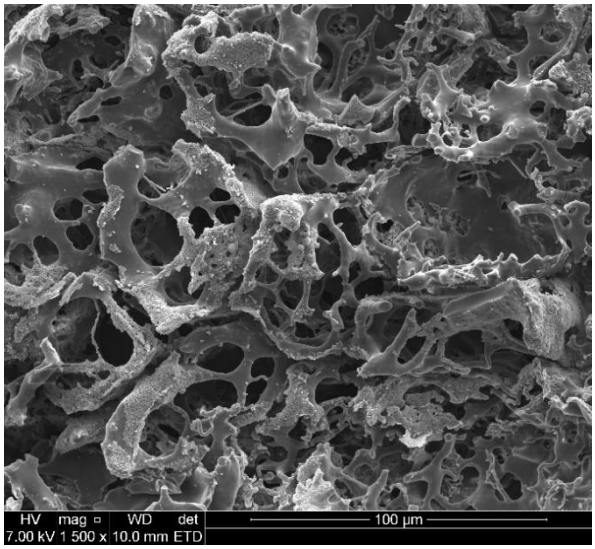

Figure 4-4: SEM of hydrochar 100 µm

Comparing the visible surfaces of the hydrochar with the feedstock, there is a clear distinction that can be observed. The surface of the hydrochar can be observed in Figure 4-2 and Figure 4-4. In the feedstock no visible pore structures can be observed. In the hydrochar, however, large, and numerous pore structures can be observed. This is only a visual observation, and further analysis would have to be done to determine true characteristics of the pore structures. There is also an absence of the cellulosic fibres observed in the feedstock. This is expected as the carbonisation of the cellulosic structures occurs during the HTL process also seen in literature as with (Méndez, et al., 2014) where the same absence of fibrous structures were observed. The carbonisation of the feedstock also results in a hydrochar with uneven and rough surfaces, these irregular and deformed surfaces are due to the volatilisation of organic components during HTL (Jaiswal, et al., 2021). The large amount of fractured and irregular structures in figure 4-2 indicates the presence of amorphous carbon (Farobie, et al., 2022). EDX analysis showed mineral deposits mainly consisting of calcium 1.3%, magnesium 0.1%, and potassium 0.3%.

4.2.5 Mineral composition of hydrochar

X-ray power diffraction (XRD) and x-ray fluorescence (XRF) analysis was done on the hydrochar to investigate the mineralogy and minerals present in the hydrochar. The comparison between the XRD done on the hydrochar obtained from the two different solvents were very similar. The XRD results of the hydrochar produced with sewage as a solvent are given in figure 4-5 and the XRD of hydrochar produced with deionised water as solvent can be seen in Annexure B. Both

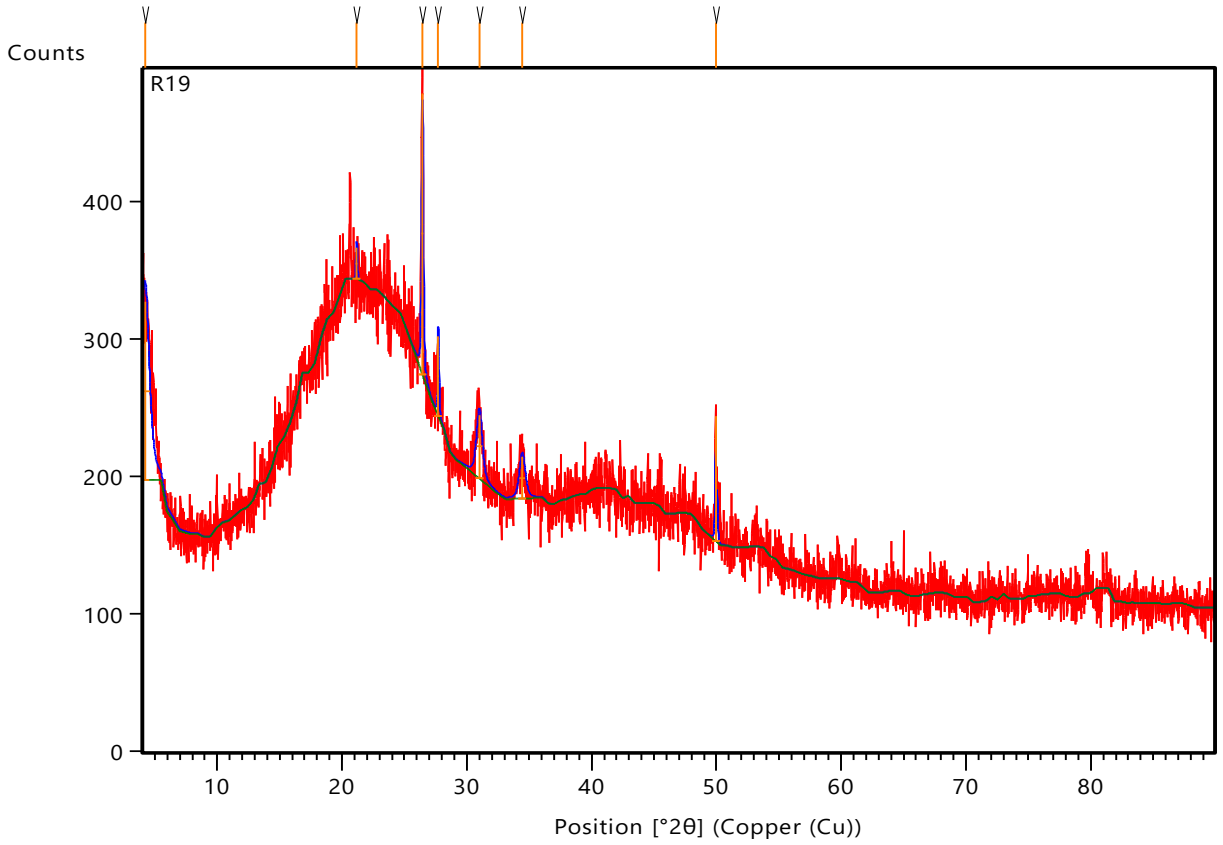

Figure 4-5: XRD of sewage hydrochar

scans were similar in nature and mineral composition and the identified minerals are given in table 4-8.

In Figure 4-5 the main broad peak at 2θ = 15-30˚ indicates a mixture of amorphous and crystalline carbon with randomly oriented aromatic sheets (Dehkhoda, et al., 2014). The sharpness of the peak is influenced by crystalline carbon structures (Kang, et al., 2018). Sharp peaks observed at 26˚ and 30.5˚ can be associated with quartz constituents (Dehkhoda, et al., 2014). Calcite is also observed from various peaks. The sharp and narrow peaks at 27˚, 34.5˚ and 50˚ are attributed to

calcite in the hydrochar. The XRD shows that the hydrochar produced is rich in high presence of quartz and calcite.

Table 4-8: Identification of peaks in XRD analysis

Diffraction peak	Mineral Content
Broad peak 15˚-30˚	Amorphous Carbon (Dehkhoda, et al., 2014)
21˚	Graphite (Siburian, et al., 2017)
26˚	Silicon dioxide (Liu, et al., 2012)
29˚	Calcite (Dehkhoda, et al., 2014)
34.5˚	Cellulose crystallization peaks (Wang, et al., 2022)

The XRF analysis supported the observations from the XRD and further showed that the hydrochar was rich in mineral components. The general composition of the XRF results is given below in Table 4-9. As supported by the XRD and EDX analysis the main make-up of the hydrochar consisted of calcite and quartz. A high amount of phosphorus containing species was found in the hydrochar. Phosphorus is abundant in food waste. Li, et al. (2020) calculated a loss of 420,400 tons of phosphorus across China's food supply chain in 2015. It is understandable that the hydrochar derived primarily from food waste would have large amounts of phosphorus present. The XRF further supports previous analyses showing other mineral constituents present in the hydrochar. This can be observed with the high quantities of calcium oxide and silicon dioxide.

Table 4-9 : XRF analysis of hydrochar

Solvent	CaO (wt.%)	SiO_2 (wt.%)	P_2O_5 (wt.%)	Al_2O_3 (wt.%)	Fe_2O_3 (wt.%)	K_2O (wt.%)	MgO (wt.%)	Na_2O (wt.%)	SO_3 (wt.%)
Sewage	30.2	25.7	20.2	4.8	1.1	4.0	3.2	0.9	3.5
Deionised water	29.4	27.6	19.0	4.6	1.4	4.7	4.4	0.9	2.7

These contents are from the XRF analysis done on the ash of the hydrochar produced. A slight increase in both P_2O_5 and SO_3 can be observed between the two different solvent runs. The higher sulphur content is likely due to the sewage as solvent as sewage contains significant amounts of sulphur. Sewage sludge contains concentrations of 0.3-2.3 wt% of sulphur as found by Dewil, et al., 2008. The overall high phosphorous content is likely attributed to the organic feedstock used during the HTL process, as described earlier by (Li, et al., 2020) high amounts of phosphorous are attributed to organic waste. The slight increase in phosphorous from the sewage run is also likely due to the high amount of phosphorous present in human waste. In the United Kingdom, sewage accounts for roughly 70% of phosphorous sources entering rivers and water bodies (Bunce, et al., 2018).

A better reflection would be the amount of sulphur present in the hydrochar of the two different chars produced. The calculation of sulphur present in the hydrochar produced with deionised water as solvent was 0.10 wt% and the sulphur present in the hydrochar produced with sewage as a solvent was 0.18 wt%. This can be compared to a low sulphur coal source, coal sources containing less than 1% sulphur are classified as low-sulphur coal sources (Chou, 2012). Sources with sulphur between 1-3% are classified as medium-sulphur coal and above 3% as high sulphur coal (Chou, 2012). The XRF analysis showed that

4.2.6 Functional group analysis

FTIR analysis was used to investigate and determine the surface functional groups present in the hydrochar. The spectra for both hydrochars produced from different solvents and the feedstock is shown in Figure 4-6 and a summary of the allocation of peaks identified is given in Table 4-10 below.

Table 4-10: Functional groups present in hydrochar

Wavelength (cm^{-1})	Allocation of bond	Functional group
3600-3200, 1370, 1020, 1210	C-O and O-H	Hydroxyl groups, alkanes, carboxylic acid and phenolics (Dehkhoda, et al., 2014)
1580, 1700	C-C	Aromatic acidic groups in ring mode (Dehkhoda, et al., 2014)
614, 545	O-P-O	Bend vibration associated with phosphates (Wang, et al., 2016)
950-1200	C-O-C and C-O-H	Glycosidic bonds associated with polysaccharides (Jiao, et al., 2018)
2850 and 2900	C-H	Aliphatic CH_2 and CH3 bonds (asymmetric and symmetric) associated with hydrocarbons
470, 1100-1000	Si-O-Si	Siloxane functional groups (Qian, et al., 2016)
2700-2400	C-H	Aromatic bonds such as ketones, aldehydes, esters, and carboxylic acids (Dehkhoda, et al., 2014)

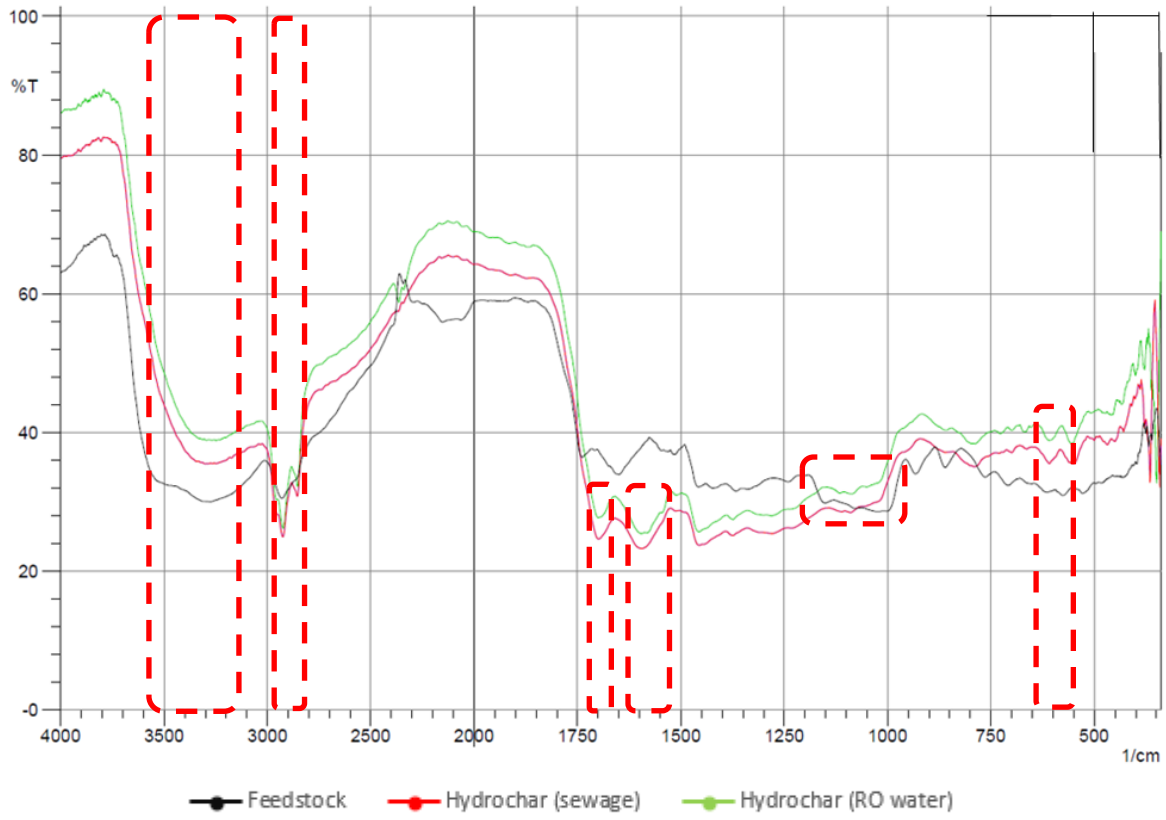

Figure 4-6 FTIR spectra of feedstock and hydrochar

The broad peak seen between 3600-3200 cm^{-1} represents the stretching of hydroxyl groups, specifically that of cellulose and together with the peaks at 2900 cm^{-1} that show C-H stretching of free sugars in the feedstock (Jiao, et al., 2018). The peaks at 2900 cm^{-1} intensify in the hydrochar and are instead attributed to C-H stretching associated with hydrocarbons.

The peaks observed at 1580 and 1700 cm^{-1} are attributed to the C-C stretch and aromatic acidic groups (Dehkhoda, et al., 2014). It is observed that aromatics are formed during the HTL process as these peaks are absent in the feedstock spectra observed in the 1500-1700 cm^{-1} range. The small narrow peaks observed at 614 and 545 cm^{-1} are associated with that of phosphates (Wang, et al., 2016). It supports the XRF analysis, and they become more prominent in the hydrochar as they are oxygenated during the HTL process. The broad band between 1200-950 cm^{-1} is attributed to glycosidic bonds (C-O-C and C-O-H) and associated with polysaccharides present in the

feedstock (Jiao, et al., 2018). This band is less intense in the hydrochar spectra due to the conversion of sugars during the HTL process.

4.2.7 Aqueous phase analysis

The aqueous phase product produced during the hydrothermal liquefaction runs was investigated and analysed. The analysis gives insight into the organic and inorganic compounds present in the aqueous phase.

4.2.7.1 Total phenols and HPLC of aqueous phase

The total phenol analysis was done on all the aqueous phases produced from the different solvent runs. The total phenols for the aqueous phase produced from the deionized water run was 2.93 g/L and for the sewage run 3.17 g/L. The amount of phenol present in the aqueous phase is high considering the U.S. Environmental Protective Agency (EPA) has declared a safe limit discharge of 0.5 parts-per-million (ppm) in effluent wastewater (Yi & Kun-Lin, 2021). An even lower limit of 1 part-per-billion is declared for drinking water. High phenol levels are common in oil refining and petrochemical industries and common in the HTL process (Yi & Kun-Lin, 2021).

The HPLC phenolic analysis quantified the specific phenolics present in the aqueous phase. Many of these phenolics present in the aqueous phase are valuable and very sought after in various industries, phenols that can be extracted are used for the production of dyes, antioxidants, pigments, alkyl phosphate, formaldehyde and urea resins, and resol resins (Swetha, et al., 2021). In Table 4-12 the various phenolics that are present in the aqueous phase are presented.

Table 4-11: HPLC of aqueous phase

Compound	Aqueous phase using deionised water as solvent	Aqueous phase using sewage as solvent
Vanillyl alcohol (p-VA) (g/kg feed)	1.96	1.68
Resorcinol (g/kg feed)	1.95	1.91
Catechol (g/kg feed)	0.22	0.19
Vanillin (g/kg feed)	0.11	0.09
Phenol (g/kg feed)	0.48	0.38
Syringol (g/kg feed)	0.51	0.30
Guaiacol (g/kg feed)	0.25	0.17

There was little notable difference between the phenolics present in the aqueous phase of the different solvent type runs and this is supported since phenols are not overwhelmingly present in sewage or domestic wastewater. Phenols are rather associated with the pharmaceutical, petrochemical, agrochemical, and plastic manufacturing industries (Yi & Kun-Lin, 2021). Swetha, et al. (2021) concluded that not many reports discuss the production of chemicals from HTL aqueous phase although the potential for the various chemicals contained with the aqueous phase should not be overlooked.

4.2.7.2 Inductively coupled plasma optical emission spectrometry

The inorganic compounds from the aqueous phase were determined by means of the ICP-OES analysis. Table 4-12 gives the inorganic compounds quantified by the ICP-OES analysis.

Table 4-12: ICP analysis of aqueous phase

Compound	Concentration water run (ppm)	Concentration sewage run (ppm)
Calcium (Ca)	2330	2290
Potassium (K)	3818	3536
Magnesium (Mg)	262	321
Sodium (Na)	504	581

As discussed earlier with the hydrochar nitrogen, phosphorus and potassium are the three major inorganic compounds used in commercial fertilizers. The aqueous phase produced during the hydrothermal liquefaction runs was in the range of 3-5 g/L which corresponds to literature of 1-8 g/L of potassium in HTL aqueous phase (Swetha, et al., 2021). From all the aqueous phase analyses done, no remarkable difference was observed between the different solvents used namely the deionized water and sewage.

HTL aqueous phase is considered a valuable byproduct of the HTL process (Swetha, et al., 2021). As discussed earlier, the main components of fertilizers are nitrogen, phosphorous and potassium and HTL aqueous phase contains these crucial components that make up liquid fertilizer (Swetha, et al., 2021). The HTL aqueous phase produced contained high amounts of potassium as well as nitrogen in the aqueous phase. Ammonia is easily recovered via stripping, but the extraction of potassium is challenging, and more research is needed in this regard (Swetha, et al., 2021). This could be extended to researching on the removal of other unwanted organic and inorganic compounds from the aqueous phase (Swetha, et al., 2021). One possible use of the AP could be that of a liquid fertilizer.

The biological analysis of the HTL aqueous phase identified and quantified the bacterium present in the primary sewage and in the post HTL aqueous phase. During HTL some of the bacteria present was completely killed off like Salmonella. Other bacteria like Escherichia coli (E.coli) was not completely killed off and was present in the aqueous phase. This should be a consideration when using primary sewage during the HTL process. Staphylococcus aureus (S.aureus) was also identified in both the sewage and HTL aqueous phase.

4.2.8 Bio-oils produced and comparison

The final product evaluated from the two different solvent type runs was the bio-oil that was produced. The bio-oil produced was evaluated mainly by means of GC-MS analysis, FTIR, elemental analysis, calorific value analysis and proximate analysis. The moisture of the oil was evaluated using the Karl Fischer titration principle.

4.2.8.1 Bio-oil physiochemical properties

The bio-oil obtained from the different solvent runs was analysed to investigate if the solvent had any adverse effect on the quality of the bio-oil from the HTL procedure. It has already been discussed and concluded that the solvent type did not influence the yield of the bio-oil.

Table 4-13: Proximate analysis comparison of bio-oil

	Bio-oil from deionized water as solvent	Bio-oil from primary sewage as solvent
Ash (g/100g Feedstock)	0.03 ± 0.02	0.06 ± 0.02
Moisture (g/100g Feedstock)	1.22 ± 0.04	1.81 ± 0.02
Volatile matter (g/100g Feedstock)	11.37 ± 0.05	13.02 ± 0.01

The higher heating value of the bio-oil is shown in Table 4-14.

Table 4-14: HHV of bio-oil compared to feedstock

	Feedstock	Deionized water	Primary sewage
Higher heating value (MJ/kg)	18.4	32.1	32.2

The typical range for the HHV of bio-oil is 30.8-42.2 MJ/kg which is lower than crude oil (Xu & Li, 2021). The bio-oil produced from the two different solvents did not have any notable difference in HHV or in carbon, nitrogen, and hydrogen content. The carbon, nitrogen and hydrogen content

of the bio-oils are given in table 4-15. The energy retention parameter of the bio-oil produced was 0.23 for both bio-oils produced with different solvents namely deionised water and sewage.

Table 4-15: Elemental analysis comparison of Bio-oils produced with different solvents

	Bio-oil with solvent deionised water	Bio-oil with solvent primary sewage
Carbon (%C)	68.2 ± 0.1	68.1 ± 0.1
Hydrogen (%H)	5.6 ± 0.2	6.0 ± 0.1
Nitrogen (%N)	3.3 ± 0.5	3.4 ± 0.1
Residual (%R)	25.85 ± 0.19	22.54 ± 0.21

GCMS was used to identify various compounds in the oil but not to quantify them. The following fatty acid esters were identified in the biocrude oil produced. These included: methyl tetradecanoate, dodecanoic acid methyl ester, hexadecenoic acid methyl ester, methyl stearate, and pentadecanoic acid 14-methyl methyl ester. Phenol compounds identified were phenol, phenol 2-methoxy, phenol 4-ethyl-2-methoxy, and phenol 2,6-dimethoxy.

4.2.9 Final remarks on water versus sewage as solvent

Using the different solvents during the hydrothermal liquefaction process had an insignificant influence on the products and their quality. Specifically, the hydrochar produced had no significant difference. The amount of sulphur present in the hydrochar amounted to 0.18 wt%. It is comparative to low sulphur coal sources which are classified as coal with less than 1% sulphur content (Chou, 2012). The small difference in solvent type can be observed in the ash content of the hydrochars produced. The primary sewage only contains 2.25% solids, and this appears in the products after HTL. Nitrogen, phosphorus potassium are three major inorganic compounds that are used in the agricultural industry as commercial fertilizers (Swetha, et al., 2021). The hydrochar had a NPK ratio of 1:1.3:1 which hints at the possibility of the hydrochar as a soil remediation product. The macronutrients present in the hydrochar increase soil nutrients and thus improve plant growth and produce yield (Agbede, 2021). NPK ratios come in various ranges and determine what the fertilizer or soil enhancers use is (Agbede, 2021).. The high aromaticity of the hydrochar produced also increases the time it takes for the hydrochar to biodegrade and thus the carbon retention is higher than non-carbon treated soils (Agbede, 2021).

The following section briefly discusses the influence of reaction time and temperature on the HTL process and the products.

4.3 Influence of temperature and reaction time on hydrochar

Section 4.3 and section 4.4 investigates the influence of reaction temperature and reaction time on the products from HTL of municipal solid waste with primary sewage as solvent.

The influence of time and temperature on the hydrochar was investigated by doing various runs and changing of the temperature and reaction time parameters. A run was done at 260˚C and for 15 minutes retention time. The hydrochar produced at these parameters had not undergone carbonisation to the extent of the hydrochars produced at higher temperatures and longer reaction times. The difference can be seen with the naked eye as the char produced is browner in colour due to not have undergone carbonisation to the extent that the hydrochar had at higher temperatures, similar observations were made in woody biomass in Saito, et al. (2018).

The change in temperature as discussed earlier with the XRD and elemental analysis increased the carbon content of the hydrochar as seen in Figure 4-7.

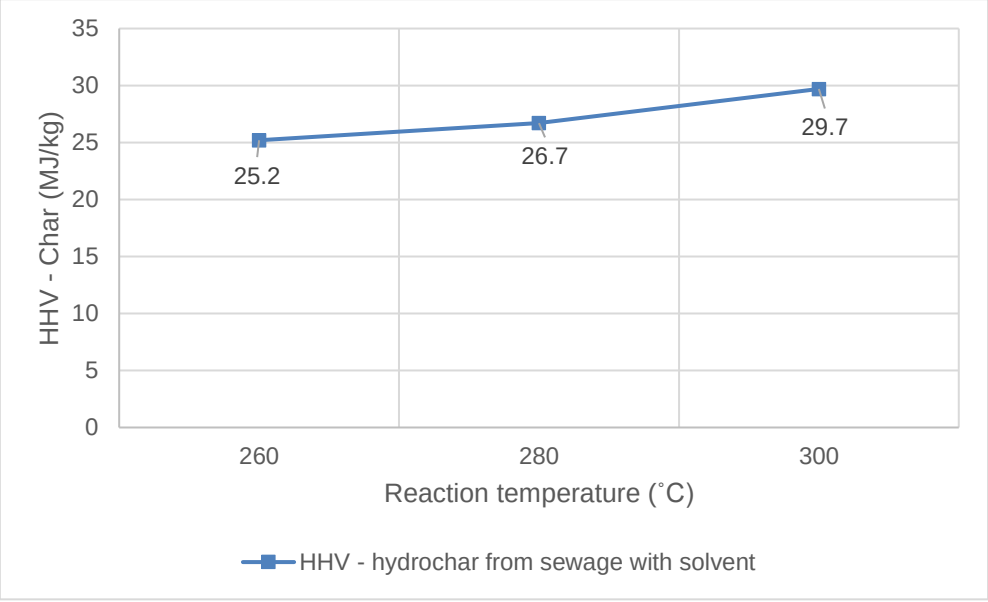

Figure 4-7: HHV of hydrochar with change in temperature

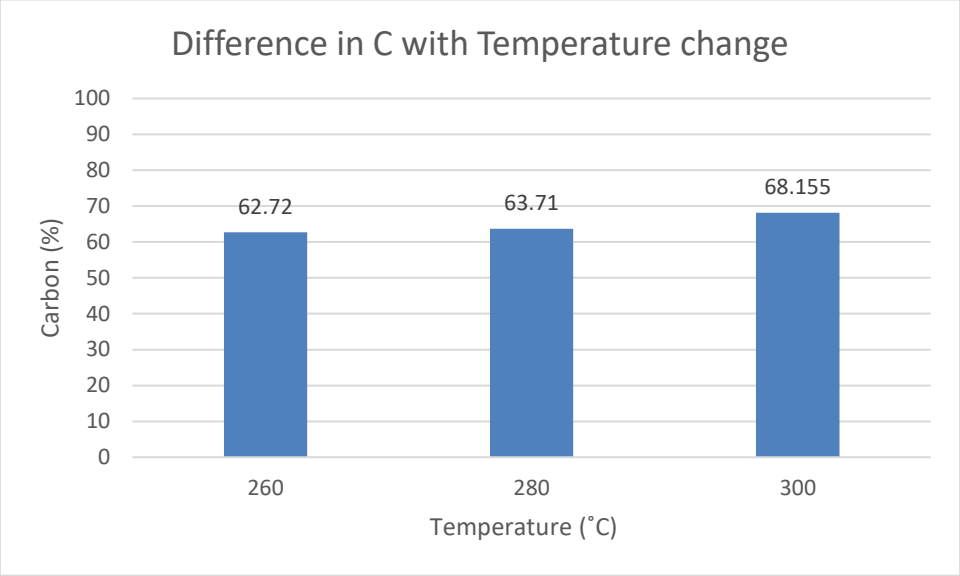

Figure 4-8: Carbon% from elemental analysis with change in temperature

The temperature increase had a clear rise in the percentage carbon in the hydrochar. A higher temperature did, however, change the yield of the hydrochar. As shown in Figure 4-8 below, an increase in temperature led to a decrease in hydrochar yield. This is supported by literature as a change in the temperature and reaction time parameters might channel more water-soluble products to the oil and gas production pathways (Miao, et al., 2012) and hence produce less hydrochar. At higher temperatures polymers, including lignin, degrade and therefore the solid-solid conversion reactions do not occur as readily reducing the production of hydrochar

(Ponnusamym, et al., 2020). The increase in temperature further upgraded the hydrochar and resulted in a slightly higher heating value for hydrochars produced at higher temperatures.

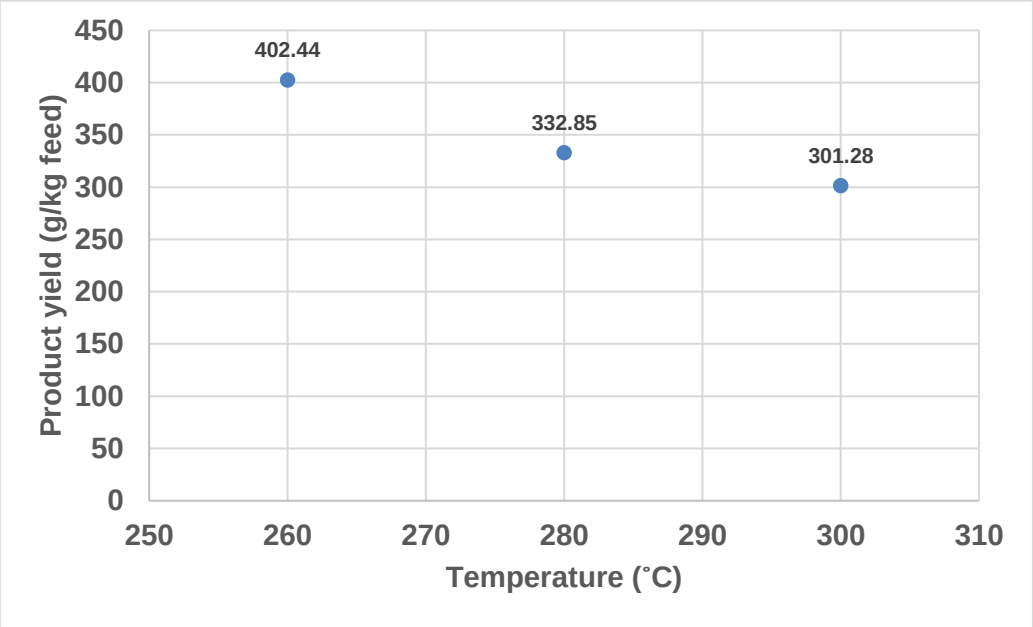

Figure 4-9: Influence of temperature on hydrochar yield

The XRD of the hydrochar produced under lower temperatures and shortened reaction time can be seen in Figure 4-9. As previously described the broad peak between 2θ = 15-30˚ is due to a mixture of crystalline and amorphous carbon structures in the sample (Dehkhoda, et al., 2014). The intensity of the peak being attributed to the amount of crystalline carbon present (Kang, et al., 2018). The broad peak between 2θ = 15-30˚ is not as broad as the peak in Figure 4-10 but it is greater in intensity. The less intense peak of hydrochar produced at higher reaction temperature and longer reaction time is an indication of less crystalline structures in the carbon mixture (Kang, et al., 2018).

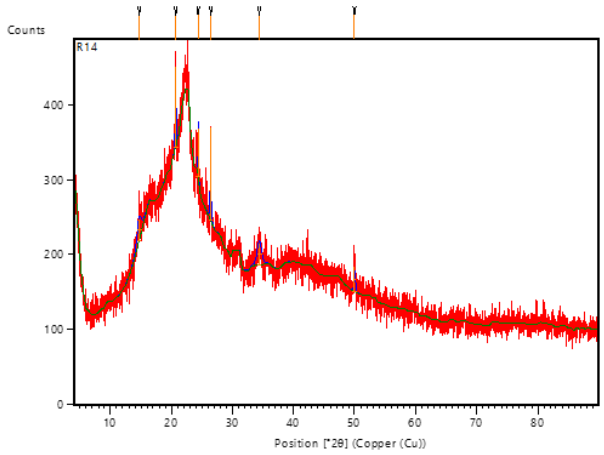

Figure 4-10: XRD of hydrochar produced at 260˚C and 15 minutes

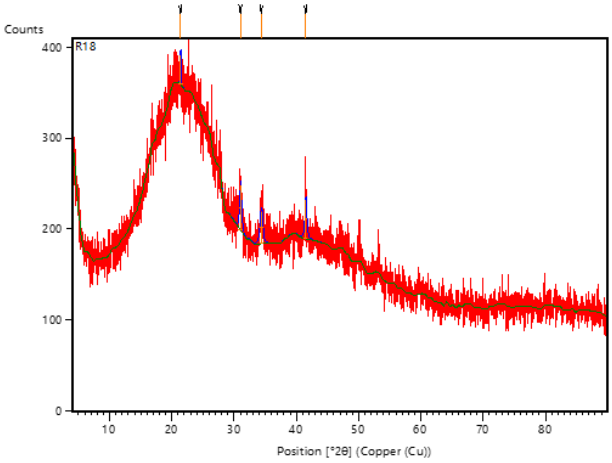

Figure 4-11: XRD of hydrochar produced at 300˚C and 60 minutes

Observing the SEM images of the hydrochars produced at different temperatures the irregular and broken structures that can be seen in the hydrochar are due to the volatilisation of organic components and the release of moisture (Farobie, et al., 2022). The hydrochar consists of a mixture of crystalline and amorphous carbon which was also observed by Wang, et al. (2022). Observing figure 4-11 and figure 4-12 can be seen that the hydrochar produced at low temperature (260˚C) and at a short retention time (15 minutes) seems to be more crystalline in nature compared to the char produced at a higher temperature (300˚C) and longer reaction time (60 minutes) which appears to be more amorphous in nature. The structure remains broken and irregular irrespective of the temperature or time.

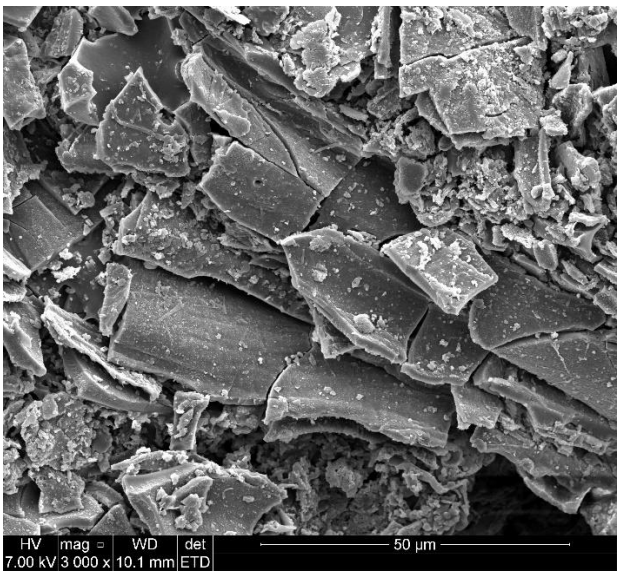

Figure 4-12: SEM of hydrochar produced at 260˚C and 15 minutes

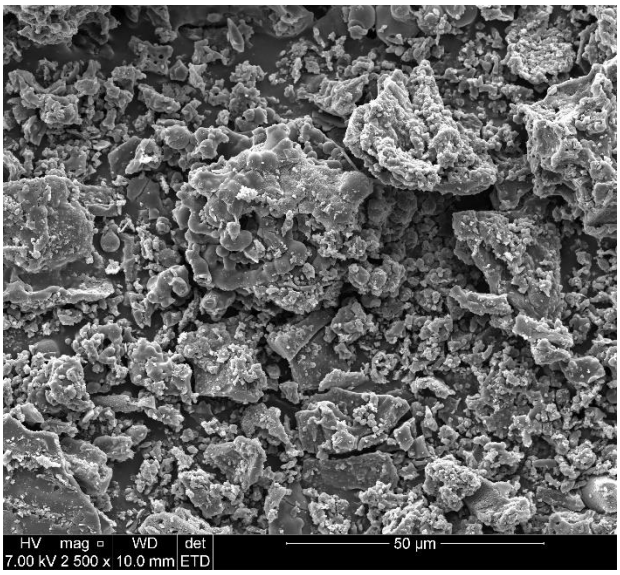

Figure 4-13: SEM of hydrochar produced at 300˚C and 60 minutes

The proximate analysis also supports the release of volatile and moisture content under higher reaction time and temperature. The moisture content for the respective runs is given in table

Table 4-16: Volatile and moisture content of hydrochars various parameters

	Hydrochar at 260˚C and 15 minutes	Hydrochar at 300˚C and 60 minutes
Volatiles (wt. %)	60.5 ± 0.6	48.4 ± 0.6
Moisture (wt. %)	3.7 ± 0.4	3.1 ± 0.5

The functional group analysis done by FTIR was compared between hydrochar produced at low temperature (260˚C) and at a short retention time (15 minutes) with hydrochar produced at a higher temperature (280˚C) and the same reaction time as well as hydrochar produced at a higher temperature (280˚C) and longer reaction time (60 minutes).

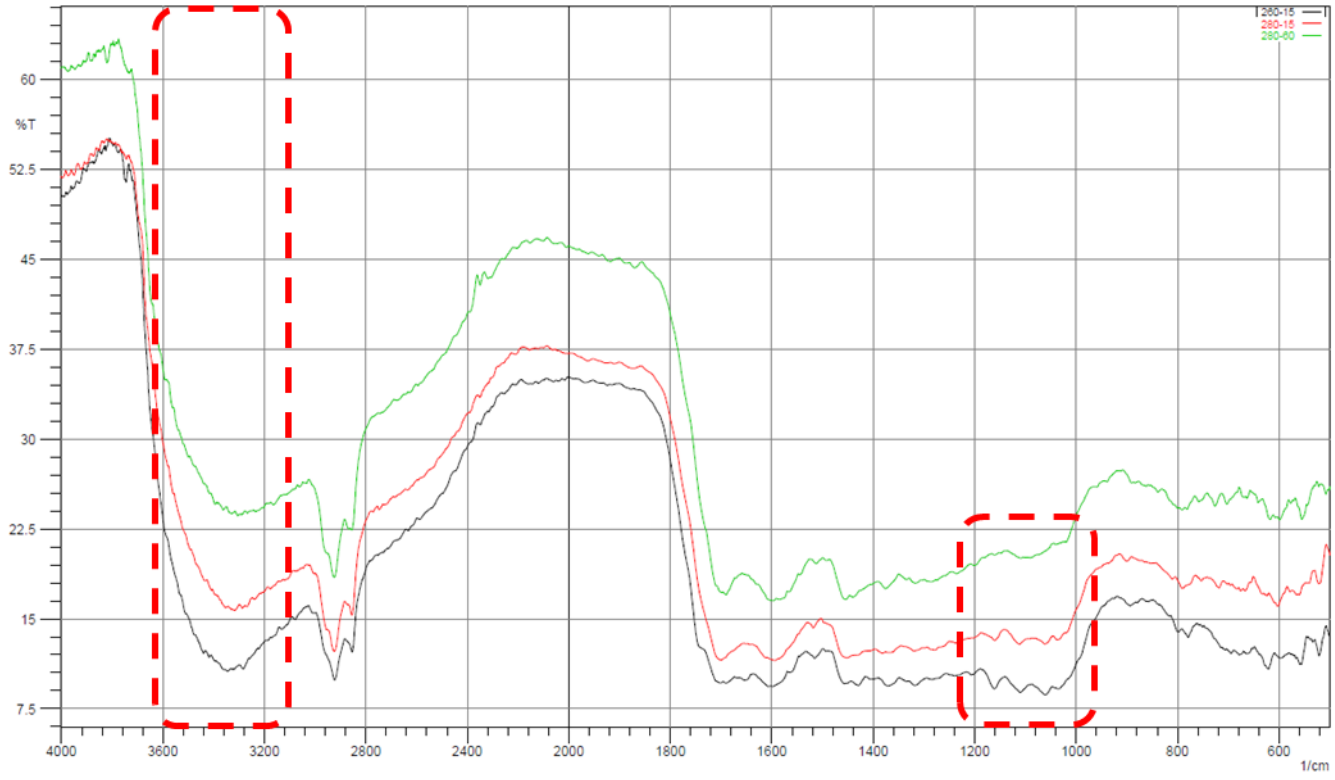

Figure 4-14: FTIR spectra of hydrochar under different reaction conditions

These spectra can be seen in Figure 4-12. The first major notable difference is the broad peak between 3600-3200 cm^{-1} representing the stretching of hydroxyl groups specifically that associated with cellulose (Jiao, et al., 2018). It is noted that as the temperature increases from 260˚C to 280˚C, this peak stretches more and becomes less intense. An increase in the carbonisation of the biomass influences this peak to become less prominent (Jiao, et al., 2018). This therefore further supports the previous hypothesis that incomplete carbonisation of the hydrochar occurs at lower temperatures. When further comparing the peaks at 280˚C with reaction time of 15 minutes and 60 minutes, this peak further stretches, showing more complete carbonisation of the cellulose. The small peaks between 1200-950 cm^{-1} associated with glycosidic bonds also becomes less prominent as the temperature and time is increased. This is contributed to the polysaccharides that get converted during the HTL process (Jiao, et al., 2018).

4.4 Influence of temperature and reaction time on bio-oil and aqueous phase

The change in reaction temperature was observed in the yield and quality of the bio-oil and aqueous phase. The increase in reaction temperature had a positive influence in the bio-oil yield. The energy retention parameter was also positively influenced with an increase in reaction temperature. Table 4-18 gives the yield, HHV and energy retention parameter of the bio-oil obtained at different reaction temperatures.

Table 4-17: Bio-oil properties from HTL at different reaction temperatures

	Bio-oil from 260 and 15 min	Bio-oil from 280 and 15 min	Bio-oil from 300 and 15 min
Yield (g/kg feed)	132.18	135.60	137.50
Higher heating value (MJ/kg)	19.3	28.9	32.2
Energy retention parameter	0.14	0.21	0.23

Very few studies include the influence of temperature on the composition of the aqueous phase and regularly only report on the influence on yield (Swetha, et al., 2021). Table 4-18 gives a comparison of the HPLC analysis of the AP at different temperatures.

Table 4-18: HPLC of AP from HTL at different reaction temperatures

Compound	AP of HTL using sewage as a solvent at 280˚C and 60 min	AP of HTL using sewage as a solvent at 300˚C and 60 min
Vanillyl alcohol (p-VA) (g/kg feed)	4.74	1.87
Resorcinol (g/kg feed)	2.61	1.16
Catechol (g/kg feed)	0.37	0.27
Vanillin (g/kg feed)	0.17	0.09
Phenol (g/kg feed)	0.78	0.63
Guaiacol (g/kg feed)	0.51	0.38

The increase in temperature led to a decrease in the phenolics detected in the HPLC of the AP. It is reported that HTL under low temperature and short retention time yields higher aqueous phase because of the reduced depolymerisation reaction (Sundar, et al., 2021). At higher reaction temperatures and longer reaction times N-containing and O-containing compounds are transformed into other products these are typically furfurals, phenols, furans, and fatty acid amides (Sundar, et al., 2021). This observation holds true as the increase in bio-oil yields are observed in table 4-18. The decrease in phenolics in the AP with an increase in reaction time was also observed, this can be seen in table 4-20.

Table 4-19: HPLC of AP from HTL at different residence times

Compound	AP of HTL using sewage as a solvent at 300˚C and 45 min	AP of HTL using sewage as a solvent at 300˚C and 60 min
Vanillyl alcohol (p-VA) (g/kg feed)	3.70	1.87
Resorcinol (g/kg feed)	1.45	1.16
Catechol (g/kg feed)	0.46	0.27
Vanillin (g/kg feed)	0.15	0.09
Phenol (g/kg feed)	0.75	0.63
Guaiacol (g/kg feed)	0.73	0.38

During the hydrothermal liquefaction of OFMSW and primary sewage temperature and reaction time played an influence on the product yields and quality.

5 Conclusions & Recommendations

5.1 HTL of organic waste with primary sewage

This study investigated the hydrothermal liquefaction of municipal solid waste and the effect that primary sewage as a solvent had on the product yields and quality. Using primary sewage as solvent during the HTL process did not have a significant effect on the product yields but exhibited some minor effects on the quality of the products. The hydrochar yields were very similar (300.1 g/kg feed) for deionised water and (301.1 g/kg feed) for sewage as solvent. The hydrochar produced was slightly higher in ash content (4.1 ± 0.8) for deionised water and (5.1 ± 0.2) for sewage. This is likely due to the solids present in the sewage (0.48 mass%) and becomes evident when conducting an ash balance. The calorific value differed only slightly. The energy retention parameter of hydrochar obtained from HTL of OFMSW and both solvents was similar, 0.50 for deionised water and 0.48 for sewage as a solvent. The calorific value of the hydrochar produced is comparable to high grade coal and the sulphur content was low enough (0.18 wt%) to be considered as a low sulphur fuel source (less than 1 wt%). The study showed that it is possible to use sewage to replace water as solvent type during the HTL process and the influence it has on the products specifically the hydrochar. This is greatly beneficial to save water during the process. The treatment of sewage will have to be further investigated to ensure microbiological content is satisfactory to health and safety standards.

5.2 Hydrochar application

As discussed throughout the literature study there are many applications for hydrochar that is produced from HTL. It is recommended and alluring to study these possible applications of hydrochar produced from HTL of OFMSW and sewage in future studies. The high calorific value of the hydrochar together with the low sulphur and ash values makes it a possible renewable fuel source and it is recommended that a techno-economic analysis be done regarding this. The high calorific value is comparable or slightly better than high grade coal. The NPK ratio of 1:1.3:1 together with the porous nature and high mineral content of the hydrochar suggests that it could also be used for soil remediation.

It is recommended that this should be investigated to establish how well the hydrochar does perform as a soil amendment. It is also recommended that hydrochar is investigated on its potential use as an adsorbent. The high amount of functional and oxygenated groups present, as

well as the porous nature of the hydrochar, allures to its adsorbent capabilities. However, these capabilities should be investigated further.

References

Abomohra, A. E., Jin, W., Tu, R., Han, S., Eid, M., & Eladel, H. (2016). Microalgal biomass production as a sustainable feedstock for biodiesel:Current status and perspectives. *Renewable and suistainable energy reviews, 64*, 596-606.

Adedeji, O. M., Russack, J. S., Molnar, L. A., & Bauer, S. K. (2022). Co-Hydrothermal Liquefaction of Sewage Sludge and Beverage Waste for High-Quality Bio-energy Production. *Fuel, 324*, 124757. doi:10.1016/j.fuel.2022.124757

Agbede, T. M. (2021). Effect of tillage, biochar, poultry manure and NPK 15-15-15 fertilizer, and their mixture on soil properties, growth and carrot (Daucus carota L.) yield under tropical conditions. *Heliyon, 7*, e07391. doi:10.1016/j.heliyon.2021.e07391

Agegnehu, G., Srivastava, A. K., & Bird, M. I. (2017). The role of biochar and biochar-compost in improving soil quality and crop performance: A review. *Applied Soil Ecology, 119*, 156-170.

Akhtar, J., & Amin, N. (2011). A review on process conditions for optimum bio-oil yield in hydrothermal liquefaction of biomass. *Renewable and Sustainable Energy Reviews, 15*, 1615-1624.

Alburquerque, J. A., Calero, J. M., Barrón, V., Torrent, J., del Campillo, M. C., Gallardo, A., & R., V. (2014). Effects of biochars produced from different feedstocks on soil properties and sunflower growth. *J. Plant Nutrit. Soil Sci., 177*, 16-25.

Alper, K., Wang, Y.-Y., Tekin, K., Meng, X., Karagoz, S., & Ragauskas, A. J. (2021). Use of a Lewis acid, a Brønsted acid, and their binary mixtures for the hydrothermal liquefaction of lignocellulose. *Fuel, 304*, 121398.

Appels, L., Baeyens, J., Degreve, J., & Dewil, R. (2008). Principles and potential of the anaerobic digestion of waste-activated sludge. *Progress in Energy and Combustion Science, 34*(6), 755-781.

Archer, E., Landman, W., Malherbe, J., Tadross, M., & Pretorius, S. (2019). South Africa's winter rainfall region drought: A region in transition? *Climate Risk Management, 25*, 100188.

Arun, J., Varshini, P., Prithvinath, P. K., Priyadarshini, V., & Gopinath, K. P. (2018). Enrichment of bio-oil after hydrothermal liquefaction (HTL) of microalgae. *Bioresource Technology, 261*, 182-187.

Ayeleru, O. O., Ntuli, F., & Mbohwa, C. (2016). Characterisation of Fruits and Vegetables Wastes in the City of Johannesburg. *World Congress on Engineering and Computer Science.* San Francisco: WCECS.

Barreto, R. A. (2018). Fossil fuels, alternative energy and economic growth. *Economic Modelling, 75*, 196-220.

Basu, P. (2010). *Biomass Gasification and Pyrolysis: Practical Design and Theory.* Elsevier.

Bauer, S. K., Reynolds, C. F., Peng, S., & Colos, L. M. (2018). Evaluating the Water Quality Impacts of Hydrothermal Liquefaction Assessment of Carbon, Nitrogen, and Energy Recovery. *Bioresource Technology Reports, 2*, 115-120.

Biswas, B., Kumar, A. A., Bisht, Y., Krishna, B. B., Kumar, J., & Bhaskar, T. (2021). Role of temperatures and solvents on hydrothermal liquefaction of Azolla filiculoides. *Energy, 217*, 119330.

Bitton, G. (2011). *Wastewater Microbiology* (4th ed.). New Jersey: Wiley-Blackwell.

Bridgewater, A. V. (2003). Renewable fuels and chemicals by thermal processing of biomass. *Chemical Engineering Journal*, 87-102.

Buchun, S., Jiaming, L., Zhangbing, Z., Mengmeng, S., Jianwen, L., Na, D., & Yuanhui, Z. (2018). Inhibitors degradation and microbial response during continuous. *Science of the Total Environment*, 1124-1132.

Bunce, J. T., Ndam, E., Ofiteru, I. D., Moore, A., & Graham, D. W. (2018). A Review of Phosphorus Removal Technologies and Their Applicability to Small-Scale Domestic Wastewater Treatment Systems. *Frontiers in Environmental Science, 6*. doi:10.3389/fencs.2018.00008

Carpio, R. B., Zhang, Y., Kuo, C.-T., Chen, W.-T., Schideman, L. C., & de Leon, R. (2021). Effects of reaction temperature and reaction time on the hydrothermal liquefaction of demineralized wastewater algal biomass. *Bioresource Technology Reports, 14*, 100679.

Chen, H.-Y., Ng, K. K., Lee, C.-H., Chen, T.-Y., Hong, P.-K. A., Yang, P.-Y., & Lin, C.-F. (2018). Entrapped biomass for removal of organics and total nitrogen fromanaerobic reactor effluents. *Bioresource Technology, 267*, 642-649.

Chou, C.-L. (2012). Sulfur in coals: A review of geochemistry and origins. *International Journal of Coal Geology, 100*, 1-13.

Correa, D. F., Beyer, H. L., Possingham, H. P., Thomas-Hall, S. R., & Schenk, P. M. (2017). Biodiversity impacts of bioenergy production: Microalgae vs. first generation biofuels. *Renewable and Sustainable Energy Reviews, 74*, 1131-1146.

Dai, Y., Zhang, N., Xing, C., Cui, Q., & Sun, Q. (2019). The adsorption, regeneration and engineering applications of biochar. *Chemosphere, 223*, 12-27.

Dandamudi, K. P., Mathew, M., Selvaratnam, T., Muppanemi, T., Seger, M., Lammers, P., & Deng, S. (2021). Recycle of nitrogen and phosphorus in hydrothermal liquefaction biochar. *Resources, Conservation & Recycling, 171*, 105644.

DEA, D. o. (2000-2010). *GHG Inventory for South Africa.* DEA.

DEA, D. o. (2018). *South Africa State of Waste Report.*

Dehkhoda, A. M., Ellis, N., & Gyenge, E. (2014). Electrosorption on activated biochar: Effect of thermo-chemical activation treatment on the electric double layer capacitance. *Applied Electrochemistry*, 141-157.

Dewil, R., Baeyens, J., Roels, J., & Van De Steene, B. (2008). Distribution of Sulphur Compounds in Sewage Sludge Treatment. *Environmental Engineering Science, 25*(6). doi:10.1089/ees.2007.0143

Du, B., Yu, Z., Tian, Y., & Ma, X. (2021). Effects of baking soda on Co-hydrothermal carbonization of sewage sludge and Chlorella vulgaris: Improved the environmental friendliness of hydrochar incineration process. *Journal of Environmental Chemical Engineering, 9*, 106404.

Dussadee, N., Unpaprom, Y., & Rmaraj, R. (2016). *Advances in Silage Production and Utilization.* InTech. doi:10.5772/61574

Elliot, D. C., Biller, P., Ross, A. B., Schmidt, A. J., & Jones, S. B. (2015). Hydrothermal liquefaction of biomass: Developments from batch to continuous process. *Bioresource Technology, 178*, 147-156.

Fan, Y., Hornung, U., & Dahmen, N. (2022). Hydrothermal liquefaction of sewage sludge for biofuel application: A review on fundamentals, current challenges and strategies. *Biomass and Bioenergy, 165*(106570).

Farobie, O., Anis, L. A., Fatriasari, W., Karimah, A., Nurcahyanil, P. R., Rahman, D. Y., . . . Aziz, M. (2022). Simultaneous production of nutritional compounds and hydrochar from Chlorella pyrenoidosa via hydrothermal process. *Bioresource Technology Reports, 20*, 101245.

Glaser, B., Haumaier, L., Guggenberger, G., & W., Z. (2001). The Terra Preta phenomenon −a model for sustainable agriculture in the humid tropics. *Naturwissenschaften, 88*, 37-41.

Gollakota, A. R., Kishore, N., & Gu, S. (2018). A review on hydrothermal liquefaction of biomass. *Renewable and Sustainable Energy Reviews, 81*(1), 1378-1392.

Gundupalli, M. P., & Bhattacharyya, D. (2021). Hydrothermal liquefaction of residues of Cocos nucifera (coir and pith). *Energy, 236*, 121466.

Hietala, D. C., & Savage, P. E. (2021). A molecular, elemental, and multiphase kinetic model for the hydrothermal. *Chemical Engineering Journal, 407*, 127007.

Hognon, C., Delrue, F., Texier, J., Grateau, M., Thiery, S., Miller, H., & A., R. (2015). Comparison of pyrolysis and hydrothermal liquefaction of Chlamydomonas reinhardtii. Growth studies on the recovered hydrothermal aqueous phase. *Biomass Bioenergy, 73*, 23-31.

Hu, C., Yan, B., Wang, K.-j., & Xiao, X.-m. (2018). Modeling the performance of anaerobic digestion reactor by the anaerobic digestion system model (ADSM). *Journal of Environmental Chemical Engineering, 6*(2), 2095-2104.

Huang, H.-j., Yuan, X., Li, B.-t., Xiao, Y.-d., & Zeng, G.-m. (2014). Thermochemical liquefaction characteristics of sewage sludge in different organic solvents. *Journal of Analytical and Applied Pyrolysis, 109*, 176-184.

Ishimura, Y., & Takeuchi, K. (2019). The spatial concentration of waste landfill sites in Japan. *Resource and Energy Economics, 58*, 101121.

Jaiswal, K. K., Kumar, V., Verma, R., Verma, M., Kumar, A., Vlaskin, M. S., . . . Kim, H. (2021). Graphitic bio-char and bio-oil synthesis via hydrothermal carbonization-co-liquefaction of microalgae biomass (oiled/de-oiled) and multiple heavy metals remediations. *Journal of Hazardous Materials, 409*, 124987.

Jatoi, A. S., Shah, A. A., Ahmed, J., Rahman, S., Sultan, S. H., Shah, A. K., . . . Murtaza, M. (2022). Hydrothermal Liquefaction of Lignocellulosic and Protein-Containing Biomass: A Comprehensive Review. *Catalyst*, 12.

Jianyun, Z., Caihui, G., Hui, Z., Shuigen, Z., Wenyan, Y., Junlong, Z., . . . Christie, P. (2017). Mechanism and effects of biochar application on morphology and migration of heavy metals in contaminated soil. *Journal of Zhejiang A&F University, 34(3)*, 543-551.

Jiao, Y., Kuang, H., Hu, J., & Chen, Q. (2018). Structural characterization and anti-hypoxia activities of polysaccharides from the sporocarp, fermentation broth and cultured mycelium of Agaricus bitorquis (Quél.) Sacc. Chaidam in mice. *Journal of Functional Foods, 51*, 75-85.

Kang, D.-S., Lee, S.-M., Lee, S.-H., & Roh, J.-S. (2018). X-ray diffraction analysis of the crystallinity of phenolic resin-derived carbon as a function of the heating rate during the carbonization process. *Carbon Letters, 27*, 108-111.

Karagoz, S., Bhaskar, T., Muto, A., & Sakata, Y. (2005). Comparative studies of oil compositions produced from sawdust, rice husk, lignin and cellulose by hydrothermal treatment. *Fuel , 84*, 875-884.

Kirsch, S. (2020). Running out? Rethinking resource depletion. *PMC7341033, 7*, 838-840.

Komilis, D., Kissas, K., & Symeonidis, A. (2014). Effect of organic matter and moisture on the calorific value of solid. *Waste Management, 34*, 249-255.

Leng, L., Yuan, X., Huang, H., Shao, J., Wang, H., Chen, X., & Zeng, G. (2015). Bio-char derived from sewage sludge by liquefaction:. *Applied Surface Science, 346*, 223-231.

Li, B., Yin, T., Udugama, I. A., Dong, S. L., Yu, W., Huang, Y. F., & Young, B. (2020). Food waste and the embedded phosphorus footprint in China. *Journal of Cleaner Production, 252*, 119909.

Liu, Y., Zhao, X., Li, J., Ma, D., & Runping, H. (2012). Characterization of bio-char from pyrolysis of wheat straw and its evaluation on methylene blue adsorption. *Desalination and Water Treatment*, 115-123.

Liu, Z., & Zhang, F.-S. (2011). Removal of copper (II) and phenol from aqueous solution using porous carbons. *Desalination, 267*, 101-106.

Liu, Z., Zhang, F.-S., & Wu, J. (2010). Characterization and application of chars produced from pinewood pyrolysis and hydrothermal treatment. *Fuel, 89*, 510-514.

Lu, X., Pellechia, P. J., Flora, J. R., & Berge, N. D. (2013). Influence of reaction time and temperature on product formation and characteristics associated with the hydrothermal carbonization of cellulose. *Bioresource Technology, 138*, 180-190.

Ma, J., Zhang, L., & Li, A. (2016). Energy-efficient co-biodrying of dewatered sludge and food waste:. *Waste Management, 56*, 411-422.

Ma, Z., Youyou, Y., Wu, Y., Xu, J., Peng, H., Liu, X., . . . Wang, S. (2019). In-depth comparison of the physicochemical characteristics of bio-char. *Journal of Analytical and Applied Pyrolysis, 140*, 195-204.

Malins, K., Kampars, V., Brinks, J., Neibolte, I., Murnieks, R., & Kampare, R. (2015). Bio-oil from thermo-chemical hydro-liquefaction of wet sewage sludge. *Bioresource Technology, 187*, 23-29.

Méndez, A., Paz-Ferreiro, J., Araujo, F., & Gascó, G. (2014). Biochar from pyrolysis of deinking paper sludge and its use in the treatment of a nickel polluted soil. *Journal of Analytical and Applied Pyrolysis, 107*, 46-52.

Mepaiyeda, S., Madi, K., Gwavava, O., & Baiyegunhi, C. (2020). Geological and geophysical assessment of groundwater contamination at the Roundhill landfill site, Berlin, Eastern Cape, South Africa. *Heliyon, 6*. doi:10.1016/j.heliyon.2020.e04249

Miao, C., Chakraborty, M., & Chen, S. (2012). Impact of reaction conditions on the simultaneous production of. *Bioresource Technology, 110*, 617-627.

Mishra, S., & Mohanty, K. (2020). Co-HTL of domestic sewage sludge and wastewater treatment derived microalgal biomass – An integrated biorefinery approach for sustainable biocrude production. *Energy Conversion and Management, 204*, 112312.

Nagasaka, C. A., Kozma, K., Brunson, K. G., Russo, C. J., Alam, T. M., & Nyman, M. (2021). Cs absorption capacity and selectivity of crystalline and amorphous Hf and Zr phosphates. *Polyhedron, 202*, 115199.

Obied, R., Smith, N., Lewis, D. M., Hall, T., & van Eyk, P. (2022). A kinetic model for the hydrothermal liquefaction of microalgae, sewage sludge and pine wood with product characterisation of renewable crude. *Chemical Engineering Journal, 428*, 131228.

Oh, D. Y., Kim, D., & Park, K. Y. (2024). A comprehensive comparative study on microwave-assisted pyrolysis products derived from raw and digested organic waste, with emphasis on sewage sludge, food waste, and livestock manure. *Heliyon*.

Olusola, O. A., Freeman, N., & Mbohwa, C. (2016). Utilization of Organic Fraction of Municipal Solid Waste (OFMSW) as Compost: A Case Study of Florida, South Africa. *World Congress on Engineering and Computer Science.* (WCECS).

Ouattara, A. D. (1997). The Challenges of Globalization for Africa. *World Economic Forum.* Harare: International Monetary Fund.

Pace, S. A., Yazdani, R., Kendall, A., Simmons, C. W., & VanderGheynst, J. S. (2018). Impact of organic waste composition on life cycle energy production, global warming and Water use for treatment by anaerobic digestion followed by composting. *Resources, Conservation & Recycling, 137*, 126-135.

Paiboonudomkarn, S., Wantala, K., Lubphoo, Y., & Khunphonoi, R. (In Press). Conversion of sewage sludge from industrial wastewater treatment to solid fuel through hydrothermal carbonization process. *Materialstoday proceedings*. doi:10.1016/j.matpr.2022.11.107.

Patra, T. K., & Sheth, P. N. (2015). Biomass gasification models for downdraft gasifier: A state-of-the-art review. *Renewable and Sustainable Energy Reviews*, 583-593.

Pham, M., Schideman, L., Sharma, B., Zhang, Y., & Chen, W.-T. (2013). Effects of hydrothermal liquefaction on the fate of bioactive contaminants in manure and algal feedstocks. *Bioresource Technology, 149*, 126-135.

Ponnusamym, V. K., Nagappan, S., Bhosale, R. R., Lay, C.-H., Nguyen, D. D., Pugazhendhi, A., . . . Kumar, G. (2020). Review on sustainable production of biochar through hydrothermal liquefaction: Physico-chemical properties and applications. *Bioresource Technology, 123414*.

Qian, L., Zhang, W., Yan, J., Han, L., Gao, W., Liu, R., & Chen, M. (2016). Effective removal of heavy metal by biochar colloids under different pyrolysis temperatures. *Bioresource Technology, 206*, 217-224.

Rajoo, K. S., Karam, D. S., Ismail, A., & Arifin, A. (2020). Evaluating the leachate contamination impact of landfills and open dumpsites from developing countries using the proposed Leachate Pollution Index for Developing Countries (LPIDC). *Environmental Nanotechnology, Monitoring & Management, 14*, 100372.

Ranjbar, S., & Malcata, F. X. (2023). Hydrothermal Liquefaction: How the Holistic Approach by Nature Will Help Solve the Environmental Conundrum. *Green Chemistry in Portugal*, 28.

Reddy, H. K., Muppaneni, T., Ponnusamy, S., Sudasinghe, N., Pegallapati, A., Selvaratnam, T., . . . Voorhies, W. D. (2016). Temperature effect on hydrothermal liquefaction of Nannochloropsis. *Applied Energy, 165*, 943-951.

Rodriguez, J. A., Filho, J. F., Melo, L. C., de Assis, I. R., & de Oliveira, T. S. (2020). Influence of pyrolysis temperature and feedstock on the properties of biochars produced from agricultural and industrial wastes. *Journal of Analytical and Applied Pyrolysis, 149*, 104839.

Saengsuriwong, R., Onsree, T., Phromphithak, S., & Tippayawong, N. (2021). Biocrude oil production via hydrothermal liquefaction of food waste in a simplified high-throughput reactor. *Bioresource Technology, 341*, 125750.

Saito, Y., Sakuragi, K., Shoji, T., & Otaka, M. (2018). Expedient Prediction of the Fuel Properties of Carbonized Woody Biomass Based on Hue Angle. *Energies, 11*(11051191).

Shafiee, S., & Topal, E. (2009). When will fossil fuel reserves be diminished? *Energy Policy, 37*(1), 181-189.

Siburian, R., Sihotang, H., Lumban Raja, S., Supeno, M., & Simanjuntak, C. (2017). New Route to Synthesize of Graphene Nano Sheets. *Oriental Journal of Chemisty, 34*, 182-187.

Silva, R. D., Shimizu, K., & Zhang, Z. (2020). Hydrothermal treatment of sewage sludge to produce solid biofuel: Focus on fuel characteristics. *Bioresource Technology Reports*, 100453.

Silva, R. D., Shimizu, K., & Zhang, Z. (2020). Hydrothermal treatment of sewage sludge to produce solid biofuel: Focus on fuel characteristics. *Bioresource Technology Reports, 11*, 100453.

Slezak, R., Unyay, H., Szufa, S., & Ledakowicz, S. (2023). An Extensive Review and Comparison of Modern Biomass Reactors Torrefaction vs. Biomass Pyrolizers. *Pyrolysis and Gasification of Biomass and Waste II)*, 2212.

Steele, M., & Schulz, N. (2012). *Water hungry coal, Burnings South Africa's water to produce electricity.* Johannesburg: Greenpeace Africa.

Suliman, W., Harsh, J. B., Abu-Lail, N. I., Fortuna, A.-M., Dallmeyer, I., & Garcia-Pérez, M. (2017). The role of biochar porosity and surface functionality in augmenting hydrologic properties of a sandy soil. *Science of The Total Environment, 574*, 139-147.

Sundar, R. P., Gopinath, K. P., Arun, J., GracePavithra, K., Joseph, A. A., & Manasa, S. (2021). Insights into valuing the aqueous phase derived from hydrothermal liquefaction. *Renewable and Sustainable Energy Reviews, 144*, 111019.

Swetha, A., ShriVigneshwar, S., Gopinath, K. P., Sivaramakrishnan, R., Shanmuganathan, R., & Arun, J. (2021). Review on hydrothermal liquefaction aqueous phase as a valuable resource for biofuels, bio-hydrogen and valuable bio-chemicals recovery. *Chemosphere, 283*, 131248.

Tang, Y., Liu, M., & Zhang, B. (2021). Can public-private partnerships (PPPs) improve the environmental performance of urban sewage treatment? *Journal of Environmental Management, 291*, 112660.

United Nations. (2015). Adoption of the Paris Agreement. Paris.

Wang, Q., Wu, S., Cui, D., Pan, S., Xu, F., Xu, F., . . . Li, G. (2022). Co-hydrothermal carbonization of corn stover and food waste: Characterization of hydrochar, synergistic effects, and combustion characteristic analysis. *Journal of Environmental Chemical Engineering, 10*(108716).

Wang, R., Lin, K., Ren, D., Peng, P., Zhao, Z., Yin, Q., & Gao, P. (2022). Energy conversion performance in co-hydrothermal carbonization of sewage sludge and pinewood sawdust coupling with anaerobic digestion of the produced wastewater. *Science of the Total Environment, 803*, 149964.

Wang, Z., Shen, D., Shen, F., & Li, T. (2016). Phosphate adsorption on lanthanum loaded biochar. *Chemosphere, 150*, 1-7.

Wu, W., Zheng, L., Shi, B., & Kuo, P.-C. (2021). Energy and exergy analysis of MSW-based IGCC power/polygeneration systems . *Energy Conversion and Management , 238*, 114-119.

Xu, Y.-H., & Li, M.-F. (2021). Hydrothermal liquefaction of lignocellulose for value-added products: Mechanism, parameter and production application. *Bioresource Technology*, 126035.

Yao, Y., Gao, B., Zhang, M., Inyang, M., & Zimmerman A., R. (2012). Effect of biochar amendment on sorption and leaching of nitrate, ammonium, and phosphate in a sandy soil. *Chemosphere, 89*, 1467-1471.

Yaseen, D. A., & Scholz, M. (2019). Textile dye wastewater characteristics and constituents of synthetic efuents: a critical review. *International Journal of Environmental Science and Technology, 16*, 1193-1226.

Yi, Z., & Kun-Lin, Y. (2021). Quantitative detection of phenol in wastewater using square wave voltammetry with pre-concentration. *Analytica Chimica Acta, 1178*. doi:10.1016/j.aca.2021.338788

Yiin, C. L., Odita, E. b., Lock, S. S., Cheah, K. W., Chan, Y. H., Wong, M. K., . . . Yusup, S. (2022). A review on potential of green solvents in hydrothermal liquefaction (HTL) of lignin. *Bioresource Technology, 364*(128075).

Yuan, P., Wang, J., Pan, Y., Shen, B., & Wu, C. (2019). Review of biochar for the management of contaminated soil: Preparation, application and prospect. *Science of The Total Environment, 659*, 473-490.

Zhao, S., & Alexandroff, A. (2019). Current and future struggles to eliminate coal. *Energy Policy, 129*, 511-520.

Zheng, J.-L., Zhu, M.-Q., & Wu, H.-t. (2015). Alkaline hydrothermal liquefaction of swine carcasses to bio-oil. *Waste Management, 43*, 230-238.

Zhou, D., SC, Z., FB, F., & Chen, J. (2012). Liquefaction of macroalgae Enteromorpha prolifera in sub-/supercritical alcohols: direct production of ester compounds. *Energy Fuels, 26*, 2342-2351.

Zhou, Y., Liu, X., Xiang, Y., Wang, P., Zhang, J., Zhang, F., . . . Tang, L. (2017). Modification of biochar derived from sawdust and its application in removal of tetracycline and copper from aqueous solution: Adsorption mechanism. *Bioresource Technology, 245*, 266-273.

Annexure A: Additional reaction information

The following reaction conditions were recorded for each run.

Run number	Solvent	Temperature (˚C)	Reaction Time (min)	Reaction pressure (MPa)
3	Deionised water	300	15	11
4	Deionised water	300	15	11
5	Primary sewage	300	15	10.8
6	Primary sewage	300	15	11
7	Primary sewage	300	30	10.4
8	Primary sewage	300	30	11
9	Primary sewage	280	15	8.3
10	Primary sewage	280	15	8.3
11	Primary sewage	280	30	8.4
14	Primary sewage	260	15	5.8
15	Primary sewage	280	45	8.9
16	Primary sewage	280	60	8.6
17	Primary sewage	300	45	10.5
18	Primary sewage	300	60	10.8
19	Primary sewage	300	15	10.5

20	Deionised water	300	15	10.4
22	Primary sewage	280	15	8.3

Annexure B: Standard operating procedure of HTL batch reactor

NORTH-WEST UNIVERSITY
YUNIBESITI YA BOKONE-BOPHIRIMA
NOORDWES-UNIVERSITEIT

SAFE WORK PROCEDURE		
1. Procedure:	**Operation of Batch Reactors**	**SWP No.: _____**
2. Scope:	**Producing Char and filtrate [solution and oil] from feedstock under pressure and at various temperatures**	**RA No.: _____**
3. Associated documents:	**HIRA**	
4. Location of Task / Equipment:	**Bio-Laboratory G09**	
5. Procedure Steps:		

Steps to follow	Control measures (Equipment / Skills / Training / Personal protective equipment requirements)
1. Place biomass and solvent into the reactor sleeve.	Use correct PPE [Gloves, lab coat and safety glasses] Extraction unit must be on and operational
2. Load the sleeve into the reactor.	Use correct PPE
3. Fit the top of the reactor to the bottom, ensuring a good seal along the gasket.	Follow Standard Procedure

4. Rotate the tope to align the markings on the top and bottom, this will correctly align the bolt holes.	Follow Standard Procedure Bolts are used maximum of three times and is discarded in the bin provided
5. Lubricate the bolts with copper slip and insert into holes.	Follow Standard Procedure
6. Tighten the bolts in a crisscross pattern using a torque wrench to 40, 60 and 70 Nm.	Use the Correct Tools for the task Use correct PPE
7. Connect the gas lines to the reactor.	Test the gas lines for leaks using the solution provided
8. Switch the extractor on	Ensure it is operational
9. Check that all connections are properly tightened	Follow Standard Procedure
10. Check that the **inlet** valve is closed.	Follow Standard Procedure
11. Open the gas supply and set the pressure to the starting pressure.	Follow Standard Procedure Test the gas lines for leaks using the solution provided
12. Check that the **outlet** valve is closed.	Follow Standard Procedure
13. Slowly open the **inlet** valve and monitor the reactor pressure.	Follow Standard Procedure
14. Slowly close the inlet valve when the desired pressure is obtained.	Follow Standard Procedure
15. Check the pressure gauge to ensure that no gas leak is present.	Follow Standard Procedure

16. Inspect all seals for integrity. (Use a diluted soap solution to check all connections and bolts for leaks.)	Follow Standard Procedure Test the gas lines for leaks using the solution provided
17. Check that the **inlet** valve is closed.	Follow Standard Procedure
18. Slowly open the **outlet** valve to purge the reactor to atmospheric pressure.	Follow Standard Procedure
19. Close the **outlet** valve	Follow Standard Procedure
20. Slowly open the **inlet** valve to pressurise reactor to starting pressure.	Follow Standard Procedure
21. Close the **inlet** valve when the starting pressure is reached.	Follow Standard Procedure
22. Attach the heating jackets to the reactor.	Follow Standard Procedure Use correct PPE Take notice of the hot surfaces
23. Ensure that all connecting wires are away from surfaces that will be heated.	Follow Standard Procedure
24. Switch on the heating jacket.	Follow Standard Procedure

25. Continuously monitor the reactor temperature and pressure until the desired conditions are reached.	Follow Standard Procedure
26. Switch off the heating jackets.	Use Correct PPE Follow Standard Procedure
27. Allow the reactor to cool to below 30 °C.	Use Correct PPE Follow Standard Procedure
28. Vent the reactor by slowly opening the **outlet** valve.	Follow Standard Procedure
29. Disconnect the gas lines from the reactor.	Follow Standard Procedure
30. Loosen the bolts in a crisscross pattern.	Follow Standard Procedure
31. Carefully remove reactor top.	Follow Standard Procedure
32. Remove the sleeve from the reactor.	Follow Standard Procedure
33. Transfer the products from the sleeve to appropriate containers.	Follow Standard Procedure
34. Clean the inside of the reactor, reactor top, gasket, and sleeve.	Follow Standard Procedure
35. Remove any debris from bolt holes.	Follow Standard Procedure
36. Complete the Logbook to record all items listed regarding the run	Follow Standard Procedure

6. Records:	• Hard copy of this safe work procedure will be available at relevant department. • Personnel performing task will undersign this safe work procedure.

SWP compiled by:	**R Bekker**
Signature:	

Designation:	**Bio-Fuel Laboratory Manager**
Date:	**26 March 2019**

Name of responsible manager:	**Prof Sanette Marx**
Signature of responsible manager:	
Designation of responsible manager:	**DST/NRF Research Chair in Biofuels**
Date:	**26 March 2019**

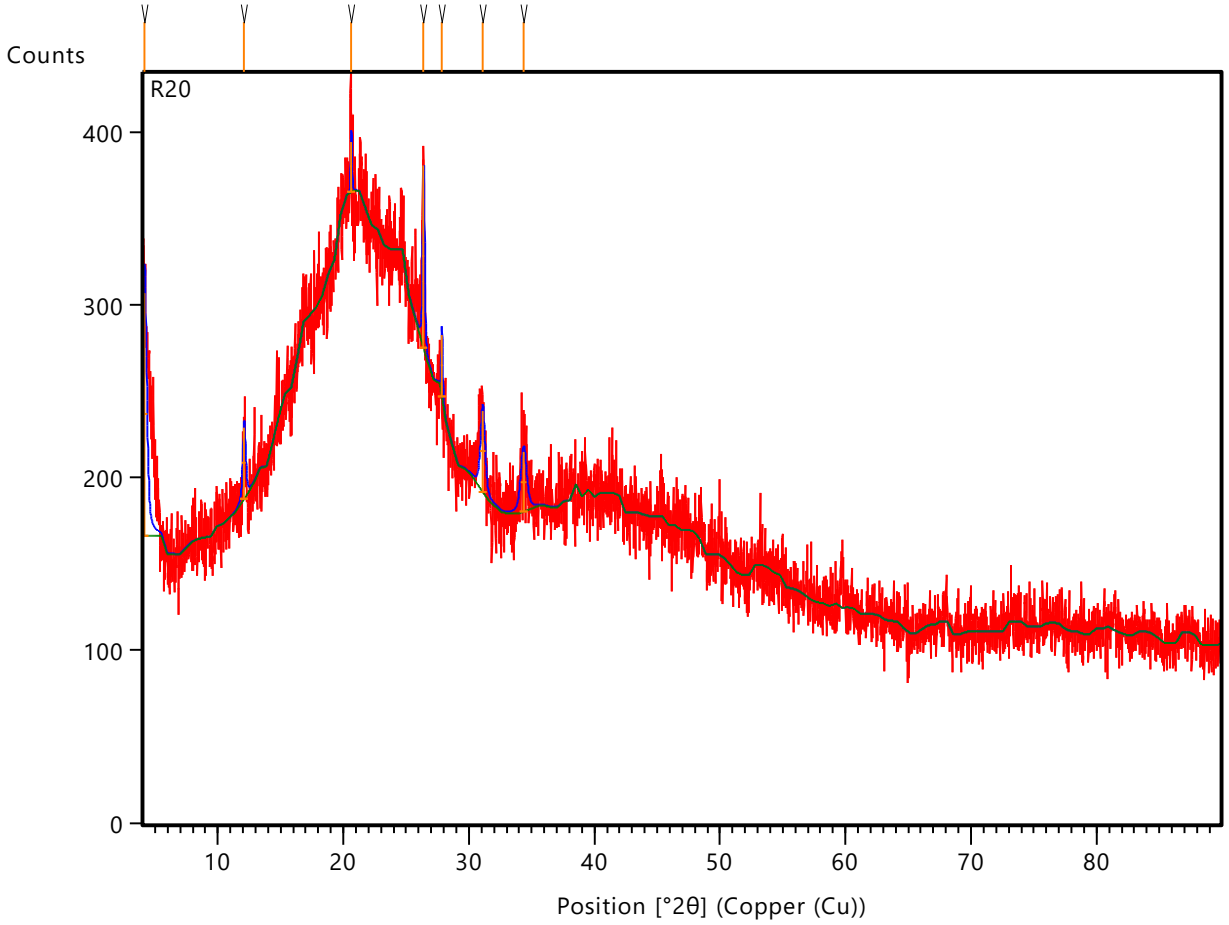

Figure B-1: XRD of deionised water run hydrochar